Int. J. Heat Mass Transfer. Vol. 16, pp. 1703–1727. Pergamon Press 1973. Printed in Great Britain

HEAT TRANSFER FROM A VIBRATING CIRCULAR CYLINDER

B. J. DAVIDSON*
School of Mathematics and Physics, University of East Anglia, Norwich, England

(*Received* 16 *August* 1971 *and in revised form* 4 *January* 1973)

Abstract—Theoretical results are obtained for heat transfer from a circular cylinder oscillating in an unbounded viscous fluid which is otherwise at rest. The amplitude of the oscillation is assumed small compared to the radius of the cylinder, which for most of the examples considered is assumed to be at a constant temperature. The analysis is based upon use of the acoustic streaming flow field and consideration is given to the cases of small and large streaming Reynolds numbers. For large streaming Reynolds numbers, a solution for the previously undetermined steady streaming flow field is computed. The results obtained cover a wide range of Prandtl number. The method of matched asymptotic expansions is exploited in the analysis and the computed results are also supplemented by an approximate method based on an integrated form of the governing equations. The relationship between the present work and other relevant contributions in the literature is discussed. In a final section, attention is devoted to a technique for determining the temperature distribution which results when a line source of heat is embedded at the centre of the oscillating cylinder.

NOMENCLATURE

a, radius of the cylinder;
k_1, k_2, conductivities of the cylinder and fluid respectively;
U_∞, typical velocity;
Q, total flux of heat per unit length from the cylinder defined in equation (35);
Pr, Prandtl number; $= \nu/\kappa$;
M, represents the ratio of a to a viscous length; $= (\omega a^2/\nu)^{\frac{1}{2}}$;
R_s, streaming Reynolds number; $= \epsilon^2 M^2 = U_\infty^2/\omega\nu$;
Nu, Nusselt number, $= Q/\pi k(\tilde{T}_\omega - \tilde{T}_\infty)$;
r, θ, cylindrical polar co-ordinates as shown in Fig. (1);
v_r, v_θ, radial and azimuthal velocities;
$u^{(s)}, v^{(s)}$, steady tangential and normal velocity components defined in equation (57);
V_∞, steady radial velocity at infinity;
Y, scaled distance co-ordinate defined in equation (27);
x, similarity variable defined in equation (50);
$\tilde{T}$, fluid temperature;
$\tilde{T}_\omega, \tilde{T}_\infty, \tilde{T}_c$, wall, ambient fluid and isothermal core temperatures respectively;
$T, T_i, \mathscr{T}, t, \tilde{t}, \hat{t}, \Theta$, dimensionless temperatures;
$G(\phi)$, dimensionless temperature on cylinder surface;
X_1, X_2, functions defined in (74);
D, function occurring in equation (84);
$b(\phi), f(\phi)$, defined in (39);
$F(x)$, function associated with the dimensionless flux of heat across a station $\theta =$ constant in the thermal boundary layer;
Q_0, function occurring in equation (80);

* Present address: Central Electricity Research Laboratories, Kelvin Avenue, Leatherhead, Surrey, England.

$g(\theta)$, function defined in equation (51);
$\bar{G}$, function associated with the finite difference form of the continuity equation, see (62);
f_0, f_1, functions occurring in equation (72);
a_n, coefficients occurring in equation (99).

Greek symbols

ν, kinematic viscosity of the fluid;
μ, coefficient of viscosity of the fluid;
κ, thermal diffusivity of the fluid;
ω^{-1}, typical time;
$\psi, \bar{\psi}, \tilde{\psi}, \varphi_{10}^{(s)}$, dimensionless stream functions;
Ψ, η, Stokes layer variables defined in equation (6);
θ, ϕ, ξ, space variables, θ defined in Fig. 1, $\phi = \theta - \pi/2$, $\xi = \phi/2$;
$\rho, \hat{\eta}, \bar{\eta}$, boundary layer distance co-ordinates;
$\Delta\xi, \Delta\bar{\eta}$, mesh lengths shown in Fig. 2;
$\bar{\eta}_\infty$, distance co-ordinate at the outer edge of a boundary layer;
ϵ, perturbation parameter; $= U_\infty/\omega a$;
$\tilde{\omega}$, perturbation parameter; $= (\epsilon^2 Pr)^{-\frac{1}{3}}$;
Ω, perturbation parameter; $= (Pr\, Rs)^{-\frac{1}{3}}$;
δ_1, displacement thickness defined in equation (65);
τ_0, shear stress defined in equation (66);
$\chi_1, \chi_2, \tilde{\chi}_1, \tilde{\chi}_2$, functions defined in equation (46) and (28);
α, constant defined in (39);
ϵ', some prescribed tolerance:
Φ, function defined in equation (98).

1. INTRODUCTION

THE PURPOSE of this paper is to examine the problem of transport of heat associated with acoustic streaming, induced by an oscillating circular cylinder, in a systematic manner and evaluate the status of existing theories. Attention has already been focused upon this particular problem, notably in the theoretical investigation and discussion on relevant experimental contributions published by Richardson [1]. However, not all of the results obtained by Richardson are correct. It is believed that the analysis described here leads to a more satisfactory understanding of the rôle played by the steady streaming velocity field in heat transfer from an oscillating cylinder, in a fluid which is otherwise at rest.

We choose a frame of reference in which the cylinder of radius a is at rest and the fluid at infinity is assumed to undergo transverse vibrations. The fluid is assumed incompressible and the flow laminar. The wall and ambient fluid are maintained at different constant temperatures in most of the cases considered here, and we restrict ourselves to small temperature differences. By suitable choice of the fluid in which the cylinder is immersed, and of the frequency of oscillation, it is possible to obtain acoustic wavelengths which are large or small compared with the cylinder radius. Attention here is confined to situations where the wavelength is large compared with the radius.

When a cylinder of radius a in a fluid of kinematic viscosity ν and thermal diffusivity κ undergoes transverse vibrations with speed $U_\infty \cos \omega t$ four length scales are important. These are the geometrical length a, the vibration amplitude U_∞/ω, the viscous length $(\nu/\omega)^{\frac{1}{2}}$ and the analogous length $(\kappa/\omega)^{\frac{1}{2}}$. From these length scales we can construct three independent parameters ϵ, M and Pr (see [2]), which charac-

terize the motion and heat-transfer properties. Thus $\epsilon = U_\infty/\omega a$ is the ratio of the vibration amplitude to the radius a, $M = (\omega a^2/\nu)^{\frac{1}{2}}$ represents the ratio of a to the viscous length and $Pr = \nu/\kappa$ is a measure of the ratio of the viscous and thermal diffusive lengths. We only concern ourselves with situations where $\epsilon \ll 1$. It is well established that if $M \gg 1$ then the first order harmonically fluctuating vorticity created at the surface of the body, which is naturally present due to the assumed oscillatory behaviour, is confined to a thin boundary layer, or Stokes layer as it is known, of thickness $0(\nu/\omega)^{\frac{1}{2}}$. Outside this layer a second order steady streaming, with characteristic velocity $O(\epsilon U_\infty)$, persists. A Reynolds number associated with this streaming is defined as (see [3]) $Rs = \epsilon^2 M^2 = U_\infty^2/\omega\nu$. The parameter Rs plays a role analogous to that of the conventional Reynolds number for steady flow past a solid body. It has been made clear by the work in reference [2] that Rs is a more fundamental parameter in these situations than M, and we adopt it as such. With $Rs \gg 1$, the outer region, away from the Stokes layer, in which the steady velocity is adjusted to zero, is of boundary-layer character with thickness $O(Rs^{-\frac{1}{2}}a)$ and for $Rs \ll 1$ the flow is Stokes-like and the adjustment takes place over a much wider region. We mention finally the dimensionless parameter k_1/k_2, where k_1, k_2 are the thermal conductivities of the cylinder and fluid respectively, which appears in the final section in association with a problem of internal heat generation. These are all the dimensionless parameters on which the subsequent theory is based.

All results which are obtained here are for $\epsilon \ll 1$ and we suppose they are asymptotically valid in the limit $\epsilon \to 0$. We formulate a theory for Rs, $Pr = O(1)$ by which we mean $\lim_{\epsilon \to 0} Pr$, $Rs = O(1)$. In the subsequent development of the theory these latter parameters may take large or small values which correspond to further limit processes in the following sense. If ϵ_1 and ϵ_2 are any two dimensionless parameters then, for example, the double-limit process $\epsilon_1 \to 0$, with $\lim_{\epsilon_1 \to 0} \epsilon_2 = O(1)$, followed by $\epsilon_2 \to \infty$ (we assume these limits apply to situations in which $\epsilon_1 \ll 1, \epsilon_2 \gg 1$) has the property that $\lim_{\epsilon_1 \to 0} \epsilon_1 \epsilon_2^\alpha = 0$ for any $\alpha > 0$ (this we assume applies to situations in which $\epsilon_1 \epsilon_2^\alpha \ll 1$). In our development of the theory, all the analysis for extreme values of the various parameters is to be interpreted in this context of ordered limit processes.

In Section 2 we formulate the general problem for $Rs = O(1)$, $Pr = O(1)$ and seek a solution of the energy equation, following a procedure used to obtain the flow field given in [2] with ϵ as a perturbation parameter, in the form of two complementary series. One series is associated with the outer region, valid at a distance $O(1)$ from the cylinder, the other with the Stokes layer. These series must match at each stage of the expansion. Pertinent results associated with the flow field are summarized, for convenience, from [2]. Following the general formulation from which equations for the steady velocity and temperature distribution in the outer region are given, we examine limiting forms of the solutions of these equations for $Rs \ll 1$, $Rs \gg 1$ since closed form solutions for $Rs = O(1)$ are not available, and the full scale numerical calculation in this situation is beyond the limitations of the available computing facility. For $Rs \ll 1$, we examine in Section 3 the cases $Pr = O(1)$, for which we show that no steady solution can exist in our unbounded region, and $PrRs = O(1)$ with particular reference to the case $PrRs \gg 1$. A feature which emerges from the analysis in Sections 2 and 3 is that for $Pr = O(1)$, or within the above framework $\lim_{\epsilon \to 0} Pr = O(1)$, the Stokes layer is so thin that it acts as a pure conduction region. The detailed flow structure of the Stokes layer plays no part in the convective heat transfer.

We show in Section 4 that for Prandtl numbers which are so large that $Pr = O(\epsilon^{-2})$ the thermal boundary layer is sufficiently thin for convection within the Stokes layer to be im-

portant. Accordingly we formulate a theory for which $\lim_{\epsilon \to 0} Pr\epsilon^2 = O(1), \lim_{\epsilon \to 0} Rs = O(1)$. However, we have been unable to draw firm conclusions about the heat-transfer characteristics in this case, where the fluid flow responsible for convection is a recirculating flow with closed streamlines.

In Section 5, the other limiting case of interest, $Rs \gg 1$, $Pr = O(1)$ is discussed. An accurate numerical method of solving the momentum and energy equations employing finite difference techniques, is described. This method is supplemented by an approximate momentum integral method which yields fairly accurate results very quickly. The details of this latter method are to be found in an Appendix to this paper. In addition to the numerical calculations, asymptotic solutions of the energy equation are found in the cases $Pr \gg 1$, $Pr \ll 1$.

The rate of heat transfer from the cylinder expressed in the form of a dimensionless quantity, the Nusselt number Nu, is determined in all cases and a critical comparison is made between the results obtained here and those derived by Richardson [1].

In the final section we employ the results derived in Section 5, for the steady streaming when $Rs \gg 1$, to study a particular problem in which the wall is no longer maintained at constant temperature. In this problem the heating is initiated by a line source of heat at the centre of the cylinder. We select this model situation as an idealization for those problems in which there is internal heat generation within the cylinder. An internal heat conduction problem must then be solved simultaneously with the external convective heat transfer problem. An iterative scheme is devised for this mixed problem which is capable of handling situations for values of the parameter $k_1 R_s^{-\frac{1}{2}}/k_2 = O(1)$. This parameter arises in the condition of continuity of heat flux across the cylinder surface and will be small compared to unity within the structure of our limit processes. Results showing the heat-transfer characteristics and the isotherms within the cylinder are presented graphically.

2. THE GOVERNING EQUATIONS

For a circular cylinder which performs transverse vibrations with speed $U_\infty \cos \omega t$ in a fluid which is otherwise at rest, we choose cylindrical polar co-ordinates fixed in the cylinder, such that the radial distance is measured from the centre of the cylinder and $\theta = 0$ coincides with the axis of oscillation as in Fig. 1.

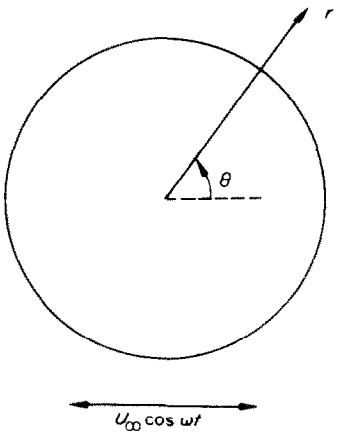

FIG. 1. The co-ordinate system.

We make all the governing equations dimensionless by using U_∞ as a typical velocity, ω^{-1} as a typical time and a, the radius of the cylinder, as a typical length. Thus the dimensionless stream function ψ, from which the radial and azimuthal velocity components are given by

$$v_r = -\frac{1}{r}\frac{\partial \psi}{\partial \theta}, \quad v_0 = \frac{\partial \psi}{\partial r}, \tag{1}$$

satisfies the equation,

$$\frac{\partial}{\partial \tau}(\nabla^2 \psi) + \frac{\epsilon}{r}\frac{\partial(\psi, \nabla^2 \psi)}{\partial(r, \theta)} = \frac{\epsilon^2}{Rs}\nabla^4 \psi. \tag{2}$$

The boundary conditions for (2) are

$$\left.\begin{aligned} &\psi = \frac{\partial \psi}{\partial r} = 0 \text{ on } r = 1, \\ &\psi \sim r \sin\theta \, e^{ir} \text{ as } r \to \infty, \end{aligned}\right\} \tag{3}$$

and the real part of any complex quantity is to be understood. In these equations, $\epsilon = U_\infty/\omega a$, $Rs = U_\infty^2/\omega\nu$, τ is the dimensionless time and the operator ∇^2 is given by

$$\nabla^2 = \frac{\partial^2}{\partial r^2} + \frac{1}{r}\frac{\partial}{\partial r} + \frac{1}{r^2}\frac{\partial^2}{\partial\theta^2}.$$

We shall be concerned entirely with the small amplitude oscillations for which $\epsilon \ll 1$. The most comprehensive description of the flow field, which owes its origins to the work of Stuart [3] and Longuet–Higgins [4] is to be found in [2]. There, with ϵ as a perturbation parameter, a solution is developed for $Rs = O(1)$, by which we mean $\lim_{\epsilon\to 0} Rs = O(1)$. The motivation for this is that Rs is a Reynolds number based on the induced steady streaming, see [3]. It is well known that a solution of (2) is not uniformly valid, and in [2] two complementary series solutions are presented, an outer solution valid at a distance $O(1)$ from the cylinder, and an inner solution valid in a Stokes shear-wave layer of thickness $O(\epsilon/Rs^{-\frac{1}{2}})$. The series solutions "match" at each stage in the manner of Van Dyke, [5]. For the details of the derivation of these solutions reference may be made to [2]; here we present the principal results. Retaining the notation of [2], the outer and inner solutions may be written as

$$\psi = \psi_{00}(r,\theta,\tau) + \frac{\epsilon}{Rs^{\frac{1}{2}}}\psi_{01}(r,\theta,\tau) + \epsilon\{\psi_{10}^{(s)}(r,\theta) + \psi_{10}^{(u)}(r,\theta,\tau)\} + O(\epsilon^2), \quad (4)$$

$$\Psi = \Psi_{00}(\eta,\theta,\tau) + \frac{\epsilon}{Rs^{\frac{1}{2}}}\Psi_{01}(\eta,\theta,\tau) + \epsilon\{\Psi_{10}^{(s)}(\eta,\theta) + \Psi_{10}^{(u)}(\eta,\theta,\tau)\} + O(\epsilon^2), \quad (5)$$

where the Stokes layer variables for the inner solutions are defined as

$$\Psi = \frac{Rs^{\frac{1}{2}}}{\epsilon\sqrt{2}}\psi, \qquad \eta = \frac{Rs^{\frac{1}{2}}}{\epsilon\sqrt{2}}(r-1). \quad (6)$$

A characteristic feature of these flows is the induced steady streaming $O(\epsilon)$, and in (4) and (5) the time-independent part of $O(\epsilon)$ has been explicitly displayed with superscript (s). For a circular cylinder, the terms displayed in (4) and (5) take the form,

$$\psi_{00} = \sin\theta\left(r - \frac{1}{r}\right)e^{i\tau},$$

$$\psi_{01} = -\sqrt{2}(1-i)\frac{\sin\theta}{r}e^{i\tau},$$

$$\psi_{10}^{(u)} = 0,$$

$$\Psi_{00} = 2\sin\theta\{\eta - \tfrac{1}{2}(1-i)(1-e^{-(1+i)\eta})\}e^{i\tau}, \quad (7)$$

$$\Psi_{01} = 2\sqrt{2}\sin\theta\{\tfrac{1}{2}(1-i)[\eta - \tfrac{1}{2}(1-i)(1-e^{-(1+i)\eta})] - \tfrac{1}{2}\eta^2 - \tfrac{1}{4}(1-i)\eta e^{-(1+i)\eta} - \tfrac{1}{4}i(1-e^{-(1+i)\eta})\}e^{i\tau},$$

$$\Psi_{10}^{(u)} = 2\sin 2\theta\left\{\frac{1}{4\sqrt{2}}(1+i)e^{-(1+i)\eta\sqrt{2}} + \frac{i}{2}\eta e^{-(1+i)\eta} - \frac{(1+i)}{4\sqrt{2}}\right\}e^{2i\tau},$$

$$\Psi_{10}^{(s)} = 2\sin 2\theta\,(\tfrac{13}{8} - \tfrac{3}{4}\eta - \tfrac{1}{8}e^{-2\eta} - \tfrac{3}{2}e^{-\eta}\cos\eta - e^{-\eta}\sin\eta - \tfrac{1}{2}\eta e^{-\eta}\sin\eta).$$

The equation, derived in [2], for $\psi_{10}^{(s)}$ is

$$\frac{1}{Rs}\nabla^4\psi_{10}^{(s)} - \frac{1}{r}\frac{\partial(\psi_{10}^{(s)}, \nabla^2\psi_{10}^{(s)})}{\partial(r,\theta)} = 0, \quad (8)$$

together with the boundary conditions,

$$\left.\begin{aligned} &\psi_{10}^{(s)} = o(r) \quad \text{as} \quad r\to\infty,\\ &\psi_{10}^{(s)} = 0\\ &\frac{\partial\psi_{10}^{(s)}}{\partial r} = -\frac{3}{2}\sin 2\theta \end{aligned}\right\} \text{on } r = 1. \quad (9)$$

We see from (8) that the steady streaming outside the Stokes layer, represented by $\psi_{10}^{(s)}$, is governed by the full equations for steady viscous flow at Reynolds number Rs. We note from (9) that the outer streaming is induced indirectly by the streaming in the Stokes layer, which is itself

a consequence of the action of Reynolds stresses. It is shown in [2] that these stresses make no direct contribution to the outer streaming. We now investigate the rôle played by this steady streaming velocity as a mechanism for convecting heat from the circular cylinder.

With the streaming Reynolds number $Rs = O(1)$ and the Prandtl number $Pr = O(1)$ where $Pr = \nu/\kappa$, the energy equation may be written in dimensionless form, with dissipative effects ignored, as

$$\frac{\partial T}{\partial \tau} + \frac{\epsilon}{r}\frac{\partial(\psi, T)}{\partial(r, \theta)} = \frac{\epsilon^2}{PrRs}\nabla^2 T, \tag{10}$$

together with the boundary conditions,

$$\begin{aligned} &T = 1 \text{ on } r = 1, \\ &T = 0 \text{ as } r \to \infty. \end{aligned} \tag{11}$$

The boundary conditions on the dimensionless temperature T defined as

$$T = \frac{\tilde{T} - \tilde{T}_\infty}{\tilde{T}_\omega - \tilde{T}_\infty}, \tag{12}$$

where $\tilde{T}$ is the temperature, are based on the assumption that the wall and ambient fluid are maintained at constant temperatures $\tilde{T}_\omega$ and $\tilde{T}_\infty$ respectively. We discuss in a later section a particular situation in which $\tilde{T}_\omega$ is not uniform. We restrict ourselves entirely to situations in which the fractional temperature difference $|\tilde{T}_\omega - \tilde{T}_\infty|/\tilde{T}_\infty$ is small compared with unity so that the dependence of the density and diffusivities upon temperature may be ignored, and the Grashof number is so small that natural convection effects may also be neglected.

As indicated earlier, we are concerned solely with small amplitude oscillations. By analogy with (4), we seek a perturbation solution of the energy equation (10) in the form

$$T = T_0 + \epsilon T_1 + \epsilon^2 T_2 + O(\epsilon^3), \tag{13}$$

where $T_i = T_i(r, \theta, Rs, Pr, \tau)$. Substituting (4) and (13) into equation (10) and successively equating coefficients of powers of ϵ we find that

$$\frac{\partial T_0}{\partial \tau} = 0, \tag{14}$$

$$\frac{\partial T_1}{\partial \tau} + \frac{1}{r}\frac{\partial(\psi_{00}, T_0)}{\partial(r, \theta)} = 0, \tag{15}$$

$$\frac{\partial T_2}{\partial \tau} + \frac{1}{r}\frac{\partial(\psi_{00}, T_1)}{\partial(r, \theta)} + \frac{1}{Rs^{\frac{1}{2}}r}\frac{\partial(\psi_{01}, T_0)}{\partial(r, \theta)} + \frac{1}{r}\frac{\partial(\psi_{10}^{(s)}, T_0)}{\partial(r, \theta)} = \frac{1}{PrRs}\nabla^2 T_0. \tag{16}$$

From (14) we deduce that T_0 has no time-dependent part, which we may intuitively expect from the assumed time-independent boundary conditions. From (7) we see that ψ_{00} and ψ_{01} vary harmonically with τ, and since T_0 is independent of time we integrate (15) once to give the form of T_1 as

$$T_1 = \phi_1(r, \theta, Rs, Pr) + \phi_2(r, \theta, Rs, Pr)\sin\tau. \tag{17}$$

Using this result, we equate separately the time dependent and time independent parts of equation (16) to yield as the equation for $T_0^{(s)}$.

$$\frac{1}{r}\frac{\partial(\psi_{10}^{(s)}, T_0^{(s)})}{\partial(r, \theta)} = \frac{1}{PrRs}\nabla^2 T_0^{(s)}. \tag{18}$$

Thus the equation for $T_0^{(s)}$ is only recovered when considering the $O(\epsilon^2)$ equation for T_2. This method of proceeding is typical for these oscillatory flow situations, as for example in [2] and [6]. We observe from equation (18) that the steady streaming velocity, governed by equation (8) plays a dominant rôle in determining the mean first order heat transfer. However, as we have already noted, equation (18) is only applicable in an outer region outside the Stokes layer. Identifying temperatures in the Stokes layer region by $\mathscr{T}(\eta, \theta, Rs, Pr, \epsilon, \tau) = T(r, \theta, Rs, Pr, \epsilon, \tau)$ and expanding $\mathscr{T}$ in an analogous manner to (13), it is easily shown that $\mathscr{T}_0^{(u)} = 0$ and that the governing equation for $\mathscr{T}_0^{(s)}$ is simply

$$\frac{\partial^2 \mathscr{T}_0^{(s)}}{\partial \eta^2} = 0. \tag{19}$$

The appropriate boundary condition is, from (11), $\mathscr{T}_0^{(s)} = 1$ on $\eta = 0$, and we require that the solution of (19) matches with the outer solution of (18). The solution of (19) correct to $O(\epsilon)$ is simply $\mathscr{T}_0^{(s)} = 1$, and we note that, to first order, the Stokes layer acts as a purely conductive region. This result is not entirely unexpected since, for $Pr = O(1)$, the thermal boundary layer is very thick compared to the Stokes layer. Under these circumstances we may expect the temperature changes across the latter to be negligible. Of course, as the Prandtl number increases the thermal boundary layer thickness decreases and in a later section we show that for Prandtl numbers for which $\epsilon^2 Pr = O(1)$, convective effects within the Stokes layer do become important.

Since, for $Rs = O(1)$, we are unable to solve equations (8) and (18) in closed form, we consider limiting forms of the solutions of (8) and (18) when $Rs \ll 1$ and $Rs \gg 1$.

3. SOLUTIONS FOR $Rs \ll 1$

We see from (8) that $Rs \ll 1$ is both a necessary and sufficient condition for the outer steady flow to be Stokes-like; the governing equation for $\psi_{10}^{(s)}$ for this case is the biharmonic equation,

$$\nabla^4 \psi_{10}^{(s)} = 0, \tag{20}$$

the solution of which must satisfy the boundary conditions (9). We note from the boundary conditions (9) that the outer steady flow has stagnation points of attachment at $\theta = \pm \pi/2$. For a direct comparison of the results obtained here with those of other authors, see for example [1], we choose as origin the stagnation point $\theta = \pi/2$, and write $\phi = \theta - \pi/2$. The solution of (20) which satisfies the boundary conditions (9) is,

$$\psi_{10}^{(s)} = -\tfrac{3}{4}(r^{-2} - 1)\sin 2\phi. \tag{21}$$

We note that (21) represents a uniformly valid solution of (20) together with (9).

We now seek solutions of the steady temperature equation (18) when $Rs \ll 1$.

Case (i): $Rs \ll 1, Pr = O(1)$

With $Rs \ll 1$ and $Pr = O(1)$ we see from the steady temperature equation (18) that diffusive effects, as well as being the dominant mode of transport in the Stokes layer, are of primary importance in the outer region. As a first approximation to $T_0^{(s)}$ we have to solve

$$\nabla^2 T_0^{(s)} = 0, \tag{22}$$

$$\left.\begin{aligned} T_0^{(s)} &= 1 \text{ on } r = 1, \\ T_0^{(s)} &= 0 \text{ as } r \to \infty. \end{aligned}\right\} \tag{23}$$

The condition at infinity follows immediately from (11) and that at $r = 1$ is the matching condition with the inner conduction solution of (19). There are no solutions of (22) which satisfy both of the conditions (23). Consequently we relax the condition at infinity on the assumption that the necessary adjustment can take place in an outer region, in which there is a balance between convective and diffusive processes. This procedure is typical for steady low Reynolds number flow past a finite body. The solution of (22) which satisfies the boundary condition at $r = 1$ is $T_0^{(s)} = 1 + B \log_e r$, where B is a constant to be determined by matching with the solution appropriate to the outer region. We assume that variables appropriate to this outer region are, by analogy with the classical Stokes–Oséen flow, of the form

$$\rho = (PrRs)^n r, n > 0, \quad t(\rho, \phi, \tau) = T(r, \theta, \tau), \tag{24}$$

where, by virtue of (21), $\psi_{10}^{(s)}$ remains $O(1)$. Using the result (21), we express equation (18) in terms of the outer "Oséen-like" variables (24) to give as the governing equation for $t_0^{(s)}$,

$$(PrRs)^{2n+1}\left[\frac{3}{2\rho^4}\sin 2\phi \frac{\partial t_0^{(s)}}{\partial \phi} + \frac{3}{2\rho^3}\cos 2\phi \frac{\partial t_0^{(s)}}{\partial \rho}\right] - (PrRs)\frac{3}{2\rho}\cos 2\phi \frac{\partial t_0^{(s)}}{\partial \rho} = \nabla_\rho^2 t_0^{(s)}, \tag{25}$$

where

$$\nabla_\rho^2 = \frac{\partial^2}{\partial \rho^2} + \frac{1}{\rho}\frac{\partial}{\partial \rho} + \frac{1}{\rho^2}\frac{\partial^2}{\partial \phi^2}.$$

We see from (25) that for no positive value of n can we achieve the necessary balance between the convective and conductive terms. We therefore conclude that no steady solutions for an unbounded medium exist for $Pr = O(1)$ and $Rs \ll 1$. Physically, the convection velocities in the proposed outer region are too weak to ever dominate diffusion. Only for the larger Prandtl numbers such that $PrRs = O(1)$ do we see that diffusive effects will become relatively less important, so that convective effects are not dominated by them everywhere. As a special case we now formulate a theory for situations where $PrRs \gg 1$, in which we show that convection, which is primarily due to the "slip-velocity" defined in (9), plays an active role.

Case (ii): $Rs \ll 1, PrRs \gg 1$

We see from (18) that as a first approximation to $T_0^{(s)}$ we may neglect the right hand side, and for the resulting equation to satisfy the condition at infinity we require that $T_0^{(s)} = 0$. Consequently we cannot match this solution with the solution $\mathcal{T}_0^{(s)} = 1$ for the Stokes layer, and so with $PrRs \gg 1$ the outer thermal region itself assumes a boundary-layer character. Substituting (21) into (18) and applying the usual boundary-layer arguments, it is easily shown that the thermal boundary layer has thickness $O[a(PrRs)^{-\frac{1}{2}}]$. We observe that the ratio of the Stokes layer thickness to this thermal boundary layer thickness is

$$\frac{\epsilon/Rs^{\frac{1}{2}}}{(PrRs)^{-\frac{1}{2}}} = \epsilon\, Pr^{\frac{1}{2}} \ll 1, \tag{26}$$

and so, although the thermal boundary layer is thin, it is still much thicker than the Stokes layer which remains essentially a conduction region. We introduce variables appropriate to the thermal boundary layer, within which the temperature is $O(1)$ and the stream function $O(\Omega)$, where $\Omega = (PrRs)^{-\frac{1}{2}} \ll 1$, as

$$t(r, \phi, \tau) = T(r, \phi, \tau),\ Y = \Omega^{-1}(r - 1),$$
$$\psi_{10}^{(s)} = \Omega \tilde{\psi}_{10}^{(s)}. \tag{27}$$

The inner expansion of the outer stream function $\psi_{10}^{(s)}$, given by equation (21), is, when written in terms of the inner variables,

$$\tilde{\psi}_{10}^{(s)} = \tilde{\chi}_1 + \Omega\tilde{\chi}_2 + O(\Omega^2), \tag{28}$$

with

$$\tilde{\chi}_1 = \tfrac{3}{2}Y \sin 2\phi,\ \tilde{\chi}_2 = \tfrac{9}{4}Y^2 \sin 2\phi.$$

We accordingly seek a perturbation solution of equation (18), expressed in terms of the thermal boundary co-ordinates (27), in the form

$$t_0^{(s)} = t_{00}^{(s)} + \Omega t_{01}^{(s)} + O(\Omega^2), \tag{29}$$

where $t_{0i}^{(s)} = t_{0i}^{(s)}(Y, \phi)$. Substituting (28) and (29) into equation (18) and equating coefficients of powers of Ω, we have as the equations for $t_{00}^{(s)}$ and $t_{01}^{(s)}$,

$$\frac{\partial(\tilde{\chi}_1, t_{00}^{(s)})}{\partial(Y, \phi)} - \frac{\partial^2 t_{00}^{(s)}}{\partial Y^2} = 0, \tag{30}$$

$$\frac{\partial(\tilde{\chi}_1, t_{01}^{(s)})}{\partial(Y, \phi)} - \frac{\partial^2 t_{01}^{(s)}}{\partial Y^2} = \frac{\partial(\tilde{\chi}_2, t_{00}^{(s)})}{\partial(Y, \phi)} + Y\frac{\partial(\tilde{\chi}_1, t_{00}^{(s)})}{\partial(Y, \phi)} + \frac{\partial t_{00}^{(s)}}{\partial Y}, \tag{31}$$

together with the boundary conditions,

$$t_{0i}^{(s)} = 0 \quad i = 0, 1 \quad \text{as} \quad Y \to \infty, \tag{32}$$

$$t_{0i}^{(s)} = \begin{cases} 1 & i = 0 \\ 0 & i = 1 \end{cases} \quad \text{on} \quad Y = 0. \tag{33}$$

The boundary conditions (32) and (33) ensure that the solution matches both with the trivial solution $T_0^{(s)} \equiv 0$, for the region outside the thermal boundary layer, and the Stokes layer solution $\mathcal{T}_0^{(s)} = 1$, respectively. It can be shown following a suitable transformation, (see [6]), that equation (30) reduces to the classical one-dimensional heat conduction equation with solution

$$t_{00}^{(s)} = 1 - \operatorname{erf}\{(\tfrac{3}{2})^{\frac{1}{2}} \cos\phi\, Y\}. \tag{34}$$

Before examining equation (31) for the higher order term $t_{01}^{(s)}$, we first determine the rate of heat transfer from the cylinder using the first

order solution (34). The total heat flux per unit length from the cylinder is

$$Q = -\int_0^{2\pi} k\left(\frac{\partial \tilde{T}}{\partial \tilde{r}}\right)_{\tilde{r}=a} a\,\mathrm{d}\phi, \tag{35}$$

where k is the conductivity of the fluid. The corresponding Nusselt number, based on the cylinder diameter and defined as

$$Nu = \frac{Q}{\pi k(\tilde{T}_\omega - \tilde{T}_\infty)}, \tag{36}$$

is given by

$$Nu = -\frac{1}{\pi}\int_0^{2\pi}\left(\frac{\partial T}{\partial r}\right)_{r=1}\mathrm{d}\phi. \tag{37}$$

From the solution (34), the corresponding Nusselt number, using (27), (29) and (37) is

$$Nu = \left(\frac{96}{\pi^3}\right)^{\frac{1}{4}}(Pr\,Rs)^{\frac{1}{2}}. \tag{38}$$

This result has also been obtained by Richardson who uses an approximate method appropriate for small Prandtl numbers. The motivation for this approach is that the thermal boundary layer, although very thin, is much thicker than the Stokes layer. However the formal procedure outlined above is more satisfactory insofar as it provides, unlike the approximate method of Richardson, a firm basis for calculating higher order terms in the Nusselt number (37). We note that for $Rs = O(1)$ and $PrRs \gg 1$, the arguments used above will again yield, to first order, the result (38) since under these circumstances the convection velocity in the thin thermal boundary layer is, to first order, simply the slip velocity in (9). Perturbations to (38) will of course depend on the detailed structure of the outer streaming which in turn depends upon Rs. For the case $Rs \ll 1$ under consideration, this structure is manifested in the thermal boundary layer by the successive terms of (28). Before considering higher order terms we note that although $PrRs \gg 1$ is a necessary condition for (38) to hold it is not, as we shall see in Section 4, a sufficient condition.

We now return to the correction of the result (38), which we calculate from the higher order term $t_{01}^{(s)}$ governed by equation (31). The solution of (31) may be expressed as

$$t_{01}^{(s)} = b(\phi)\cos\phi\,[-1 + \mathrm{erf}\{\alpha\cos\phi Y\} + \exp\{-\alpha^2 Y^2\cos^2\phi\}] + f(\phi)\cos\phi\, Y^2 \times \exp\{-\alpha^2 Y^2\cos^2\phi\}, \tag{39}$$

where

$$\alpha^2 = \tfrac{3}{2},$$

$$b(\phi) = \frac{2(6/\pi)^{\frac{1}{2}}}{3\sin 2\phi}[-\cot\phi + \phi\,\mathrm{cosec}^2\phi],$$

and

$$f(\phi) = \tfrac{1}{2}(6/\pi)^{\frac{1}{2}} \times [2\,\mathrm{cosec}^2\phi + 1 - 2\phi\cot\phi\,\mathrm{cosec}^2\phi].$$

This completes the solution (29) to $O(\Omega)$. We use this result to readily show that

$$Nu = \left(\frac{96}{\pi^3}\right)^{\frac{1}{4}}(PrRs)^{\frac{1}{2}}\left\{1 - \left(\frac{\pi}{24}\right)^{\frac{1}{4}}(PrRs)^{-\frac{1}{4}} + O[(PrRs)^{-1}]\right\}. \tag{40}$$

This constitutes the principal result for this case.

Unlike the correction of relative order $(PrRs)^{-\frac{1}{4}}$, to the Nusselt number shown in (40), Richardson obtains a correction $O(\epsilon Pr^{\frac{1}{2}})$ by a method which is not a systematic development from his first approximation. Since, as we recall from Section 1, the theory developed here, and implicitly in [1], is basically one in which $Pr = O(1)$ and $Rs = O(1)$, Richardson's correction is smaller than that shown in (40). The neglect of these more important terms by Richardson is due entirely to the fact that he ignores the influence of the structure of the outer streaming upon convective heat transfer in the thermal boundary layer.

We again recall that although the thermal boundary layer is very thin, it is much thicker

than the Stokes layer which plays the rôle of a conduction layer. We anticipate that for sufficiently large Prandtl numbers, convective effects in the Stokes layer will become important. We observe that equation (26) indicates that we may expect that the thermal and Stokes layers will have the same thickness if $\epsilon Pr^{\frac{1}{4}} = O(1)$. This leads naturally on to Section 4 where we examine the case $\lim_{\epsilon \to 0} Rs = O(1)$, $\lim_{\epsilon \to 0} \epsilon^2 Pr = O(1)$.

4. HEAT TRANSFER AT VERY LARGE PRANDTL NUMBERS

$Rs = O(1), \epsilon^2 Pr = O(1)$

For this case, as we have already anticipated, the Stokes layer will no longer play its passive conduction rôle, and convective effects will become important within it. Expressing the energy equation (10) in terms of the inner Stokes layer variables (6), then the governing equation for the temperature $\mathscr{T}$ in the Stokes layer is

$$\frac{\partial \mathscr{T}}{\partial \tau} + \epsilon\left(1 - \frac{\epsilon\sqrt{2\eta}}{Rs^{\frac{1}{4}}}\right)\frac{\partial(\psi, \mathscr{T})}{\partial(\eta, \theta)} = \frac{\epsilon^2}{2(\epsilon^2 Pr)}\frac{\partial^2 \mathscr{T}}{\partial \eta^2} + O(\epsilon^3). \quad (42)$$

We seek a perturbation solution of (42), with $\epsilon^2 Pr = O(1)$, in the form

$$\mathscr{T} = \mathscr{T}_0 + \epsilon \mathscr{T}_1 + \epsilon^2 \mathscr{T}_2 + O(\epsilon^3), \quad (43)$$

where $\mathscr{T}_i = \mathscr{T}_i(\eta, \theta, Rs, Pr, \tau)$. Substituting (43) and the expansion for Ψ given by (5), into equation (42), we equate coefficients of powers of ϵ. It can be shown, following a similar procedure to that used in deriving equation (18), that the leading term $\mathscr{T}_0$ is again time-independent and satisfies the equation,

$$\frac{\partial(\Psi_{10}^{(s)}, \mathscr{T}_0^{(s)})}{\partial(\eta, \theta)} = \frac{1}{2(\epsilon^2 Pr)}\frac{\partial^2 \mathscr{T}_0^{(s)}}{\partial \eta^2}, \quad (44)$$

where the steady Stokes layer velocity, represented by $\Psi_{10}^{(s)}$, is given by (7). This important equation shows that the thermal boundary layer now possesses a full structure on the scale of the Stokes layer.

As is well known, and can be deduced from (7), the steady part of the tangential velocity in the Stokes layer, which features in (44), undergoes a change of sign. The direction of the tangential velocity is such that at the edge of the Stokes layer, fluid is carried over the cylinder surface and out away from the cylinder along the axis of oscillation. Fluid adjacent to the cylinder surface within the Stokes layer is flowing in the opposite direction and continuity within the boundary layer is maintained by a streamline pattern in the form of closed loops.

A numerical investigation of equation (44) was attempted using a standard marching procedure, which we describe in Section 4, for $\epsilon^2 Pr = O(1)$. This method failed and its failure may be attributed to the reversed flow described above. The difficulty is analogous to that encountered when, for example, a numerical integration is attempted to advance a two-dimensional steady boundary-layer calculation past a regular separation point, and into the region of reversed flow beyond. Any numerical scheme for integrating (44) with $\epsilon^2 Pr = O(1)$ must presumably be based upon a boundary value method similar to those employed for elliptic equations. We do not pursue this point further here but consider below the special case $\epsilon^2 Pr \gg 1$, in which the thermal boundary layer is now very thin, on the Stokes layer scale, and within which the convective velocity is unidirectional. A perturbation solution, as in Section 3, is proposed. The first term of this has been obtained by Richardson [1]. However, the validity of the approach adopted as described below is questioned on account of the closed streamline nature of the Stokes layer.

$Rs = O(1), \epsilon^2 Pr \gg 1$

It can be shown that the thermal boundary layer thickness in this case is $O([Pr\epsilon^2]^{-\frac{1}{4}}a)$. Accordingly we introduce thermal boundary-layer co-ordinates ρ, t where, with $\tilde{\omega} = (\epsilon^2 Pr)^{-\frac{1}{4}}$,

$$\rho = \tilde{\omega}^{-1}\eta, \qquad t(\rho, \theta) = \mathscr{T}(\eta, \theta). \quad (45)$$

Note that since the velocity in the Stokes layer

close to the wall is in the direction of θ increasing we have, in this case, reverted to the original variable θ. The inner expansion of the stream function $\Psi_{10}^{(s)}$ expressed in terms of the inner variables ρ, θ is

$$\Psi_{10}^{(s)} = \tilde{\omega}^2\chi_1 + \tilde{\omega}^3\chi_2 + O(\tilde{\omega}^4), \qquad (46)$$

where

$$\chi_1 = \frac{\sin 2\theta}{2}\rho^2, \qquad \chi_2 = -\frac{\sin 2\theta}{3}\rho^3.$$

Thus in the thermal boundary layer we seek a perturbation solution of equation (44) in the form

$$t_0 = t_{00} + \tilde{\omega}t_{01} + \tilde{\omega}^2 t_{02} + O(\tilde{\omega}^3). \qquad (47)$$

Substituting (46) and (47) into equation (44) and equating coefficients of powers of $\tilde{\omega}$ gives as the equations for t_{00} and t_{01},

$$\frac{\partial(\chi_1, t_{0n})}{\partial(\rho, \theta)} - \frac{1}{2}\frac{\partial^2 t_{0n}}{\partial\rho^2} = -n\frac{\partial(\chi_2, t_{00})}{\partial(\rho, \theta)}, \qquad n = 0, 1. \qquad (48)$$

The boundary conditions for (48) are

$$\begin{aligned} &t_{0n} = 0 \text{ as } \rho \to \infty, \qquad n = 0, 1, \\ &t_{0n} = \begin{cases} 1 & n = 0 \\ 0 & n = 1 \end{cases} \qquad \text{on } \rho = 0. \end{aligned} \qquad (49)$$

The solution of (48) for t_{00} which satisfies (49), obtained in terms of the similarity variable

$$x = \rho/g(\theta), \qquad (50)$$

is (see [7]),

$$t_{00}(x) = \frac{1}{\Gamma(\frac{4}{3})}\int_x^\infty e^{-s^3}\,ds, \qquad (51)$$

where

$$g^3(\theta) = \tfrac{9}{2}\sin^{-\frac{1}{2}}2\theta\int_0^\theta \sin^{\frac{1}{2}}2s\,ds.$$

The expression for t_{01}, which represents the next term of the solution in our apparently self-consistent procedure, has been derived in closed form, but it is not presented here. From the two term solution (47) we calculate the Nusselt number (37), using (45), as

$$Nu = \epsilon^{-1}Rs^{\frac{1}{2}}(Pr\epsilon^2)^{\frac{1}{3}} \times \{1{\cdot}30 - 0{\cdot}30\,(\epsilon^2 Pr)^{-\frac{1}{3}} + O[(\epsilon^2 Pr)^{-\frac{2}{3}}]\}. \qquad (52)$$

As we have already mentioned, Richardson has obtained, in a slightly different but equivalent form, the solution (51) and hence the first term of the expression (52). He shows that by the introduction of a suitable numerical factor, the first term of (52) remains valid, to within a multiplicative constant, even in those cases where the Stokes layer thickness is not small compared to the diameter of the cylinder. As before his approach does not permit a systematic development of the solution for the temperature, as in (47). However we now question the relevance of the model which we have chosen to describe the temperature field, as represented by equations (45) and (47).

Consider the dimensionless flux of heat, Q, across a station θ = constant in the thermal boundary layer. This is given by

$$Q = \int_0^\infty \frac{\partial\Psi_{10}^{(s)}}{\partial\rho}t_0\,d\rho, \qquad (53)$$

$$= \tilde{\omega}^2\left[\int_0^\theta \sin^{\frac{1}{2}}2s\,ds\right]^{\frac{1}{3}}F,$$

where, to first order, $F = (\frac{9}{2})^{\frac{1}{3}}\int_0^\infty xt_{00}(x)\,dx \neq 0$.

The result (53) implies that although $Q = 0$ at the axis of oscillation $\theta = 0$, it is infinite at $\theta = \pi/2$ where the recirculating region for this first quadrant terminates. For steady flow past a finite body all this heat will be swept downstream. However in the present case we may expect the heat to be swept back along the recirculating streamlines with some, but not all, of the heat being carried away along the axis of oscillation. We may infer from the work of Grimshaw [8] that for this fluid of very small diffusivity, the recirculating Stokes layer region is at uniform

temperature $\tilde{T}_c \neq \tilde{T}_\omega, \tilde{T}_\infty$; and that this "isothermal core" region is separated from the wall and outer regions by a thin boundary layer in which the heat flux is $O(\tilde{\omega}^2)$. This model then requires the heat flux at $\theta = 0$ to be non-zero and $O(\tilde{\omega}^2)$. This result exposes the weakness of our arguments leading up to (52).

We do not pursue this theoretically interesting situation any further. In the next section we consider the heat transfer characteristics when the streaming Reynolds number $Rs \gg 1$ with $Pr = O(1)$. We note *a priori* that the Stokes layer is once more reduced to its purely conductive role. The only work which has been carried out for this case, in [1], is of a highly speculative nature.

5. SOLUTIONS FOR $Rs \gg 1$

For large values of the streaming Reynolds number, the outer steady flow governed by equation (8) assumes a boundary-layer character, the Stokes layer being then embedded within this outer boundary layer. From order of magnitude arguments, (see [3]), it can be shown that the thickness of the outer boundary layer is $O(aRs^{-\frac{1}{2}})$, or a factor $O(\epsilon^{-1})$ times thicker than the Stokes layer. It is within this outer boundary layer that the steady tangential component of velocity finally decays to zero. Accordingly, for this outer boundary layer we introduce scaled variables $\bar{\psi}$, $\bar{\eta}$ where

$$\bar{\psi}_{10}^{(s)} = Rs^{\frac{1}{2}}\psi_{10}^{(s)}, \qquad \bar{\eta} = \frac{Rs^{\frac{1}{2}}}{2}(r-1), \tag{54}$$

and for convenience, we define a space variable ξ as $\xi = \phi/2$. Consequently because of the symmetry associated with this problem, we only concern ourselves with the region $0 \leqslant \xi \leqslant \pi/4$. Expressing equation (8) in terms of the boundary layer co-ordinates (54) we see that the equation to be satisfied by $\bar{\psi}_{10}^{(s)}$ is

$$\frac{\partial\bar{\psi}_{10}^{(s)}}{\partial\bar{\eta}}\frac{\partial^2\bar{\psi}_{10}^{(s)}}{\partial\xi\partial\bar{\eta}} - \frac{\partial\bar{\psi}_{10}^{(s)}}{\partial\xi}\frac{\partial^2\bar{\psi}_{10}^{(s)}}{\partial\bar{\eta}^2} = \frac{\partial^3\bar{\psi}_{10}^{(s)}}{\partial\bar{\eta}^3}, \tag{55}$$

together with, from (9),

$$\frac{\partial\bar{\psi}_{10}^{(s)}}{\partial\bar{\eta}} = 0 \text{ as } \bar{\eta} \to \infty,$$
$$\bar{\psi}_{10}^{(s)} \sim 3\sin 4\xi\bar{\eta} \text{ as } \bar{\eta} \to 0. \tag{56}$$

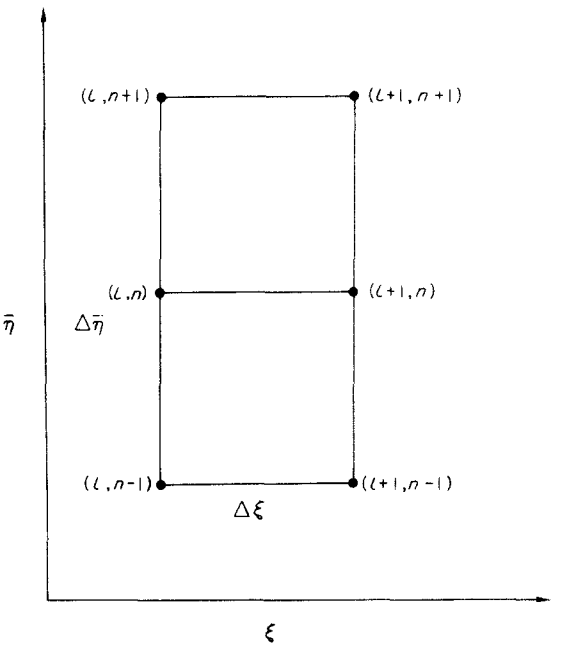

FIG. 2. The mesh with pivotal points used in the numerical integrations, $Rs \gg 1$.

The condition at infinity ensures that the steady tangential velocity component dies away to zero and the condition at $\bar{\eta} = 0$ is to be interpreted as the matching condition with the Stokes layer solution (7).

A limited study of the mechanics of this outer boundary layer has been carried out by Stuart [3] and Riley [9]. Using different methods, both these authors present results from solutions of equation (55), in the form of series about the stagnation point $\xi = 0$ of the outer steady flow. However the solution obtained by the above authors does not, for the number of terms retained in the series, satisfactorily describe the flow over the whole region $0 \leqslant \xi \leqslant \pi/4$.

In this paper we describe briefly an accurate numerical method of solving equation (55),

subject to the boundary conditions (56). Here we only outline the numerical procedure used and refer the interested reader to [10] where full details of the computation scheme may be found.

For the numerical method which was employed it is convenient to work with the steady tangential and normal velocity components, related to $\bar{\psi}^{(s)}_{10}$ as

$$u^{(s)} = \frac{\partial \bar{\psi}^{(s)}_{10}}{\partial \bar{\eta}}, \qquad v^{(s)} = -\frac{\partial \bar{\psi}^{(s)}_{10}}{\partial \xi}, \tag{57}$$

respectively. Thus, integrating (55) once with respect to $\bar{\eta}$ we have, together with the continuity equation,

$$\left.\begin{aligned} u^{(s)}\frac{\partial u^{(s)}}{\partial \xi} + v^{(s)}\frac{\partial u^{(s)}}{\partial \bar{\eta}} &= \frac{\partial^2 u^{(s)}}{\partial \bar{\eta}^2}, \\ \frac{\partial u^{(s)}}{\partial \xi} + \frac{\partial v^{(s)}}{\partial \bar{\eta}} &= 0, \end{aligned}\right\} \tag{58}$$

together with, from (56),

$$\left.\begin{aligned} &u^{(s)} = 3\sin 4\xi, \qquad v^{(s)} = 0 \text{ at } \bar{\eta} = 0, \\ &u^{(s)} = 0 \text{ as } \bar{\eta} \to \infty. \end{aligned}\right\} \tag{59}$$

We shall also require $u^{(s)} \equiv 0$ at $\xi = 0$. The problem of solving numerically the coupled set of non-linear partial differential equations (58) is reduced, using an implicit finite difference scheme, to a simple marching procedure. A double suffix notation is used as shown in Fig. 2. With $l = 1$ at $\xi = 0$ and $n = 1$ at $\bar{\eta} = 0$, then $u^{(s)}_{l,n}$ is the value of $u^{(s)}$ at the pivotal point (l, n), distant $(l-1)\Delta\xi$ from $\xi = 0$ and $(n-1)\Delta\bar{\eta}$ from $\bar{\eta} = 0$. The computation procedure enables us to evaluate $u^{(s)}$ at $(l+1, n+1)$ from a finite difference form of (58) in terms of the values at the other five grid points. The derivatives in the differential equations are replaced by first order central differences and quantities are evaluated at $[(l+\frac{1}{2})\Delta\xi, n\Delta\bar{\eta}]$. For example, the derivatives $\partial u^{(s)}/\partial\xi$ and $\partial^2 u^{(s)}/\partial\bar{\eta}^2$ in (58) are replaced by

$$\left.\begin{aligned} \left(\frac{\partial u^{(s)}}{\partial \xi}\right)_{l+\frac{1}{2},n} &= (u^{(s)}_{l+1,n} - u^{(s)}_{l,n})/\Delta\xi, \\ \left(\frac{\partial^2 u^{(s)}}{\partial \bar{\eta}^2}\right)_{l+\frac{1}{2},n} &= (\bar{u}_{n+1} - 2\bar{u}_n + \bar{u}_{n-1})/\Delta\bar{\eta}^2, \end{aligned}\right\} \tag{60}$$

where $\bar{u}_n = \frac{1}{2}(u^{(s)}_{l,n} + u^{(s)}_{l+1,n})$. The non-linear term $u^{(s)}\partial u^{(s)}/\partial\xi$ is quasilinearized so that only linear equations need be solved in each cycle of an iterative procedure which is used to solve the non-linear equations at each value of ξ. Thus, if $[u^{(s)}_{l+\frac{1}{2},n}]^{(j)}$ is the approximation used for $u^{(s)}_{l+\frac{1}{2},n}$ at the jth cycle of the iteration, then the approximation used for $[u^{(s)}(\partial u^{(s)}/\partial\xi)]_{l+\frac{1}{2},n}$ at the $(j+1)$th cycle is

$$\begin{aligned} &\left[\left(u^{(s)}\frac{\partial u^{(s)}}{\partial \xi}\right)_{l+\frac{1}{2},n}\right]^{(j+1)} \\ &= 2[u^{(s)}_{l+1,n}]^{(j)}[u^{(s)}_{l+1,n}]^{(j+1)} \\ &\qquad - [u^{(s)^2}_{l+1,n}]^{(j)} - [u^{(s)^2}_{l,n}]^{(j)} \\ &\qquad \overline{\qquad\qquad 2\Delta\xi \qquad\qquad}. \end{aligned} \tag{61}$$

The values of $v^{(s)}_{l+\frac{1}{2},n}$, which are required in the momentum equation, are obtained by writing the continuity equation in finite difference form centred upon the mid-point of the mesh $[(l+\frac{1}{2})\Delta\xi, (n+\frac{1}{2})\Delta\bar{\eta}]$. Thus

$$v^{(s)}_{l+\frac{1}{2},n+1} = v^{(s)}_{l+\frac{1}{2},n} + \bar{G}(u, \Delta\xi, \Delta\bar{\eta}), \tag{62}$$

where $\bar{G}$ involves the values of the current iterate of u at the mesh points, and $v^{(s)}_{l+\frac{1}{2},1} = 0$ by (59). Substitution of the difference approximations into the momentum equation displayed in (58), using (61) and (62) yields the following set of linear equations for the jth iterate to $u^{(s)}_{l+1,n}$ at the station $\xi = l\Delta\xi$,

$$\begin{aligned} a_n[u^{(s)}_{l+1,n+2}]^{(j)} + b_n[u^{(s)}_{l+1,n+1}]^{(j)} \\ + c_n[u^{(s)}_{l+1,n}]^{(j)} = d_n, \end{aligned} \tag{63}$$

where $n = 1, \ldots (N-1)$. The value of N is chosen so that $\bar{\eta}_\infty = N\Delta\bar{\eta}$ adequately represents the "outer edge" of the boundary layer. In (63) the coefficients a_n, b_n, c_n and d_n depend upon the known quantities $\Delta\bar{\eta}$, $\Delta\xi$, the previous iterate $[u^{(s)}]^{(j-1)}$ at the mesh points, and $v^{(s)}_{l+\frac{1}{2},n}$ calculated from (62). Thus, since from

(59) we have $u^{(s)}_{l+1,N+1} \equiv 0$, $u^{(s)}_{l+1,1} = 3 \sin(4l\Delta\xi)$, the equations (63) represent $N-1$ equations for the $N-1$ values of the jth iterate $[u^{(s)}_{l+1,2}]^{(j)} \ldots [u^{(s)}_{l+1,N}]^{(j)}$. This set of simultaneous equation (63) may be readily solved for $[u^{(s)}]^{(j)}$ at the mesh points $(l+1, n)$, $n = 1, \ldots N-1$ by triangular resolution and back substitution. The iterations through (62) and (63) were terminated when the sum of the absolute values of the differences of the quantities $u^{(s)}_{l+1,n}$ between successive iterations did not exceed some prescribed tolerance ϵ' and the values so obtained were deemed to represent the solution at that station. To advance the solution a further step $\Delta\xi$ we require starting values for the iterative scheme described above. For each value of ξ, except $\xi = 0$, the iteration was started by taking $[u^{(s)}_{l+2,n}]^{(1)} = u^{(s)}_{l+1,n}$. At the stagnation point $\xi = 0$ the solution is simply $u^{(s)} \equiv 0$. To check the accuracy of the solution obtained, various values of $\Delta\xi$, $\Delta\bar{\eta}$, N and ϵ' were used. By employing standard extrapolation formulae a solution accurate to five decimal places has been obtained.

The above finite difference scheme for the non-linear differential equations (58) consumes relatively large amounts of computer time. A complementary method based upon momentum integral techniques has been devised, which reduces the problem described above to the integration of a system of ordinary differential equations. Integrating the momentum equation in (58) from $\bar{\eta} = 0$ to $\bar{\eta} = \infty$ gives

$$\frac{\mathrm{d}}{\mathrm{d}\xi}\int_0^\infty u^{(s)2}\,\mathrm{d}\bar{\eta} = -\left(\frac{\partial u^{(s)}}{\partial \bar{\eta}}\right)_{\eta=0}. \tag{64}$$

Profiles for $u^{(s)}$ of exponential type were introduced in (64) and further details of the development of the method may be found in the Appendix to this paper.

An overall picture of the flow field may be obtained from Figs. 3–5. Figure 3 shows profiles of the velocity component $u^{(s)}$ at various stations around the cylinder. Figure 4 shows the displacement thickness, defined in our problem as

$$\frac{\delta_1(\xi)}{\{2aRs^{-\frac{1}{2}}\}} = \frac{1}{3\sin 4\xi}\int_0^\gamma u^{(s)}\,\mathrm{d}\bar{\eta}. \tag{65}$$

Included in Fig. 4, along with the value of δ_1 obtained from the finite series difference solution, are values calculated from the series solutions of Stuart [3] and Riley [9], and from the approximate momentum integral method.

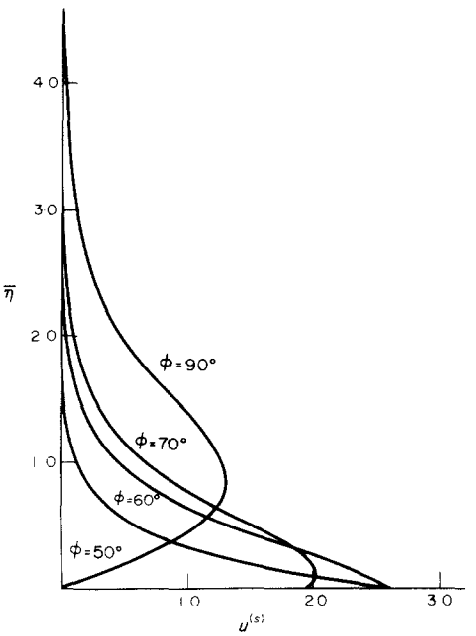

FIG. 3. Transverse velocity profiles associated with the steady streaming for $Rs \gg 1$.

The limitations of the former method and effectiveness of the latter are revealed. A similar comparison is made for the shear stress at the inner edge of the outer boundary layer. Thus if τ_0 is the shear stress,

$$\frac{\tau_0}{\left\{\dfrac{\mu U_\infty Rs^{\frac{1}{2}}}{4a}\right\}} = \left(\frac{\partial u^{(s)}}{\partial \bar{\eta}}\right)_{\bar{\eta}=0}, \tag{66}$$

where μ is the coefficient of viscosity, is shown in Fig. 5. An interesting feature of this flow, postulated in [3] and [9], is that $u^{(s)}$ is non-zero at the

axis of oscillation. From the symmetry of the problem under consideration we shall, at the axis, have a collision of boundary layers, originating from two quadrants, and fluid will be ejected along the axis in the form of a jet.

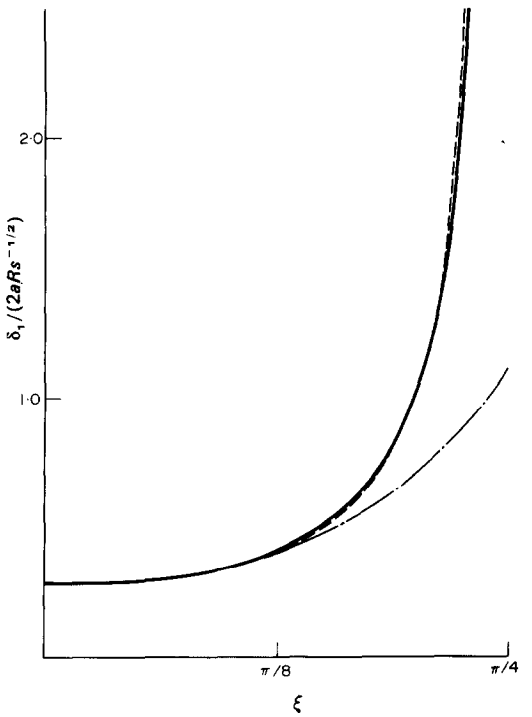

FIG. 4. The displacement thickness obtained from the finite difference, —; series, — · —; and momentum integral, — —, solutions for $Rs \gg 1$.

A theoretical and experimental study of these jet-like flows, in a variety of axi-symmetric situations will be the subject of a subsequent paper [13]. The importance of this flow structure from the present point of view is that heat which is carried over the surface of the cylinder will be swept away along the axis of oscillation, thus avoiding the difficulties encountered in the previous section.

We now employ the results derived above for the steady streaming to study the transfer of heat from the cylinder, maintained at uniform temperature, when Rs is large.

$Rs \gg 1$, $Pr = O(1)$

We identify temperatures in the outer velocity boundary layer by

$$\bar{t}(\bar{\eta}, \xi, \tau) = T(r, \theta, \tau), \tag{67}$$

where we note, from equation (54), that $\bar{\eta} = Rs^{\frac{1}{2}}(r - 1)/2$. Expressing equation (18) in terms of the boundary-layer co-ordinates (54) and (67) we find that the equation to be satisfied by $\bar{t}_0^{(s)}$ is

$$\frac{\partial(\bar{\psi}_{10}^{(s)}, \bar{t}_0^{(s)})}{\partial(\bar{\eta}, \xi)} = -\frac{1}{Pr}\frac{\partial^2 \bar{t}_0^{(s)}}{\partial \bar{\eta}^2}, \tag{68}$$

together with the boundary conditions,

$$\begin{aligned} \bar{t}_0^{(s)} &= 1 \text{ on } \bar{\eta} = 0, \\ \bar{t}_0^{(s)} &= 0 \text{ as } \bar{\eta} \to \infty, \end{aligned} \tag{69}$$

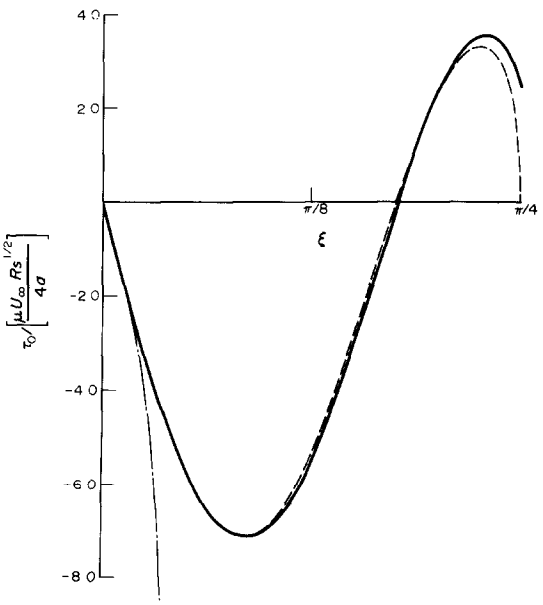

FIG. 5. The shear stress at the inner edge of the outer velocity boundary layer from the finite difference, ——; series, — · —; and momentum integral, — —, solutions for $Rs \gg 1$.

and a suitable condition on $\xi = 0$. We note again that the condition on $\bar{\eta} = 0$ ensures that the solution matches with that in the purely conductive Stokes layer.

With $\frac{\partial \bar{\psi}_{10}^{(s)}}{\partial \bar{\eta}} = u^{(s)}$ and $\frac{\partial \bar{\psi}_{10}^{(s)}}{\partial \xi} = -v^{(s)}$,

calculations for which have been carried out as described above, equation (68) lends itself readily to the finite difference scheme which was used to solve the momentum equation. As before derivatives are replaced by first order central differences. The resulting difference equations can then be expressed in an analogous form to (63) and are again solved by triangular resolution and back substitution. The boundary conditions for the resulting difference equations are (69). The initial condition which is used to start the solution at $\xi = 0$ is determined as follows. At $\xi = 0$, $u^{(s)} = 0$ and $V^{(s)}$ is given by

$$v^{(s)} = -2\sqrt{3}(1 - \exp(-2\sqrt{3}\bar{\eta})). \quad (70)$$

The solution of equation (68) for $\partial\bar{t}_0^{(s)}/\partial\bar{\eta}$ at the stagnation point $\xi = 0$ is then found to be

$$\frac{\partial\bar{t}_0^{(s)}}{\partial\bar{\eta}} = \frac{-2\sqrt{3}Pr}{M(1, 1 + Pr, Pr)} \times \exp\{-Pr[2\sqrt{3}\bar{\eta} + \exp(-2\sqrt{3}\bar{\eta}) - 1]\}, \quad (71)$$

where M is a confluent hypergeometric function, (see [11]). Equation (71) may be solved for the initial temperature distribution using a simple quadrature. Since the energy equation (68) is linear, the time taken to solve the equation over the entire field of integration is only a fraction of the time needed for the evaluation of the non-linear velocity equations (58). Thus with $u^{(s)}$ and $v^{(s)}$ determined, this technique provides a rapid and accurate method of calculating heat-transfer rates over a wide range of Prandtl numbers.

A simple approximate method has been devised, and used in conjunction with that already described in the Appendix for the momentum equation. It is based on the equation

$$\frac{\mathrm{d}}{\mathrm{d}\xi}\int_0^\infty u^{(s)}\bar{t}_0^{(s)}\,\mathrm{d}\bar{\eta} = -\frac{1}{Pr}\left(\frac{\partial\bar{t}_0^{(s)}}{\partial\bar{\eta}}\right)_{\bar{\eta}=0},$$

obtained by integrating (68) with respect to $\bar{\eta}$. Further details of the method are to be found in the Appendix. It is an efficient and accurate method over only a limited range of Prandtl number of $O(1)$.

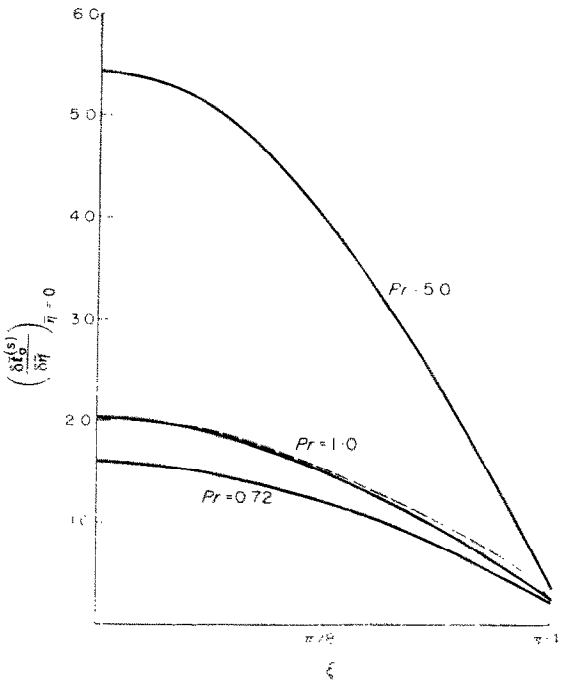

FIG. 6. The local heat transfer for $Pr = 0{\cdot}72$, $1{\cdot}0$, $5{\cdot}0$ from the finite difference solution together with the local heat transfer for $Pr = 1{\cdot}0$, – – –, derived from the momentum integral solution for $Rs \gg 1$.

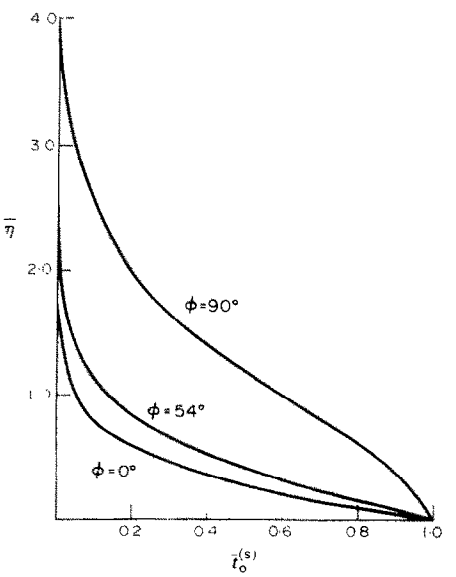

FIG. 7. Temperature profiles for $Pr = 1{\cdot}0$, $Rs = 1$.

In Fig. 6 we show the behaviour of the local heat transfer as a function of ξ for $Pr = 0{\cdot}72$, 1 and 5, based on the finite difference calculations. Included in Fig. 6 is the local heat transfer for $Pr = 1{\cdot}0$ calculated from the approximate method given in the Appendix. Figure 7 shows profiles of the temperature $\bar{t}_0^{(s)}$ at various stations around the cylinder for $Pr = 1{\cdot}0$ obtained from the finite difference method. Calculations have been carried out using the finite difference technique for the range of Prandtl numbers, $0{\cdot}2 \leqslant Pr \leqslant 10$. Outside this range the method becomes less effective due to the disparity in thickness between the thermal and velocity boundary layers. Consequently we supplement these calculations with asymptotic analyses, valid for large and small Prandtl numbers respectively.

$Rs \gg 1$, $Pr \gg 1$

When $Pr \gg 1$, the thermal boundary layer will again be so thin, relative to the outer streaming boundary layer, that we may anticipate the convection velocity within the thermal boundary layer to be, to a first approximation, simply the slip velocity in (59). We show that this is indeed the case and the result (38) for the Nusselt number obtained in Section 2 for $Rs \ll 1$, $PrRs \gg 1$, is recovered. Perturbations to the result (38), which depend upon the detailed structure of the outer streaming, will of course differ here from those calculated in Section 3.

As $\bar{\eta} \to 0$ we note that

$$\bar{\psi}_{10}^{(s)} \sim f_0(\xi)\bar{\eta} + f_1(\xi)\bar{\eta}^2 + O(\bar{\eta}^3), \qquad (72)$$

where, from (56), $f_0(\xi) = 3 \sin 4\xi$ and $f_1(\xi)$ is numerically evaluated from the velocity gradient at $\bar{\eta} = 0$ shown in Fig. 5. Applying the usual boundary-layer arguments we see that the convection and conduction terms in (68) are comparable for $Pr \gg 1$ if we set

$$\rho = Pr^{\frac{1}{2}}\bar{\eta}, \qquad \varphi_{10}^{(s)} = Pr^{\frac{1}{2}}\bar{\psi}_{10}^{(s)}, \qquad (73)$$

and

$$\hat{t}_0(\rho, \xi) = \bar{t}_0(\bar{\eta}, \xi).$$

The inner expansion of the outer stream function $\bar{\psi}_{10}^{(s)}$ expressed in terms of the "inner" variables (73) is, from (72),

$$\varphi_{10}^{(s)} = X_1 + Pr^{-\frac{1}{2}}X_2 + O(Pr^{-1}), \qquad (74)$$

where

$$X_1 = 3 \sin 4\xi\rho, \qquad X_2 = f_1(\xi)\rho^2.$$

Accordingly we seek a perturbation solution of (68) expressed in terms of the variables (73), for $Pr \gg 1$, of the form

$$\hat{t}_0^{(s)} = \hat{t}_{00}^{(s)} + Pr^{-\frac{1}{2}}\hat{t}_{01}^{(s)} + O(Pr^{-1}). \qquad (75)$$

Substituting (74) and (75) into equation (68) and equating coefficients of powers of $Pr^{-\frac{1}{2}}$, we have as the equations for $\hat{t}_{00}^{(s)}$ and $\hat{t}_{01}^{(s)}$,

$$\frac{\partial(X_1, \hat{t}_{0n}^{(s)})}{\partial(\rho, \xi)} - \frac{\partial^2 \hat{t}_{0n}^{(s)}}{\partial \rho^2} = -n\frac{\partial(X_2, \hat{t}_{00}^{(s)})}{\partial(\rho, \xi)}, \ (n = 0, 1) \qquad (76)$$

together with the boundary conditions

$$\hat{t}_{0n}^{(s)} = \begin{cases} 1 & n = 0 \\ 0 & n = 1 \end{cases} \text{ on } \bar{\eta} = 0$$
$$\hat{t}_{0n}^{(s)} = 0 \text{ as } \bar{\eta} \to \infty, \ n = 0, 1, \qquad (77)$$

and a suitable initial condition at $\xi = 0$ derived as that for $Pr = O(1)$ in equation (71). We see that the form of equation (76) for $\hat{t}_{00}^{(s)}$ is analogous to that of (30), from which we deduce the corresponding result (38) for the Nusselt number. The solution of equation (76) for $\hat{t}_{01}^{(s)}$ has been derived numerically, using the finite difference scheme described above. The Nusselt number calculated from the two term solution (75), using (54) and (73), is

$$Nu = Rs^{\frac{1}{2}}Pr^{\frac{1}{2}} \times \left\{\left(\frac{96}{\pi^3}\right)^{\frac{1}{2}} - 0{\cdot}26\, Pr^{-\frac{1}{2}} + O(Pr^{-1})\right\}. \qquad (78)$$

We see that the correction term in (78) for $Rs \gg 1$, $Pr \gg 1$ is indeed different in nature to the corresponding result (40) found in Section 3, which is valid when $Rs \ll 1$ but with $PrRs \gg 1$. We attribute this to deviations of the velocity

field from the Stokesian formula (21) when Rs is large.

$Rs \gg 1$, $Pr \ll 1$

For very small Prandtl numbers, the thermal boundary layer will be large in thickness compared with the outer velocity boundary layer and the convection–conduction balance will be found in a region where the tangential steady velocity is effectively zero. We show that in this case, in contrast to the case $Rs \ll 1$ $Pr \ll 1$ studied in Section 3 where the convection velocities were shown to be too weak to ever counteract diffusion, that the entrainment velocity, when $Rs \gg 1$, eventually dominates the outward diffusion.

As a first approximation to $\bar{t}_0^{(s)}$ we solve, from (68) with $Pr \ll 1$,

$$\left.\begin{aligned} &\frac{\partial^2 \bar{t}_0^{(s)}}{\partial \bar{\eta}^2} = 0, \\ &\bar{t}_0^{(s)} = 1 \text{ on } \bar{\eta} = 0, \\ &\bar{t}_0^{(s)} = 0 \text{ as } \bar{\eta} \to \infty, \end{aligned}\right\} \tag{79}$$

together with an initial condition which may be derived from (71). The solution of (79) which satisfies the condition on $\bar{\eta} = 0$ is

$$\bar{t}_0^{(s)} = 1 + Q_0 \bar{\eta}. \tag{80}$$

We see that we cannot satisfy the infinity condition in (79). We thus relax the infinity condition and anticipate that $Q_0(\xi)$ will be determined by matching this solution with a solution appropriate to an outer region in which there is a balance between convective and diffusive terms in (68). The scale of this outer region, where $\bar{\psi}_{10}^{(s)} = O(1)$ and $\bar{t}_0^{(s)} = O(1)$, in which convective and diffusive effects are comparable, is $O(Pr^{-1})$. Consequently we set

$$\begin{aligned} \hat{\eta} &= Pr\, \bar{\eta}, \\ \Theta(\hat{\eta}, \xi) &= \bar{t}(\bar{\eta}, \xi), \end{aligned} \tag{81}$$

and Θ satisfies

$$\frac{\partial^2 \Theta}{\partial \hat{\eta}^2} - V_\infty \frac{\partial \Theta}{\partial \hat{\eta}} = 0, \tag{82}$$

where

$$V_\infty(\xi) = -\left(\frac{\partial \bar{\psi}_{10}^{(s)}}{\partial \xi}\right)_{\bar{\eta} = \infty} < 0$$

is shown in Fig. 8. It is interesting to note that the outer velocity boundary layer under discussion in this section exists only by virtue of the fact that $V_\infty < 0$ for all ξ. This result was established by a simple argument in [9] and is

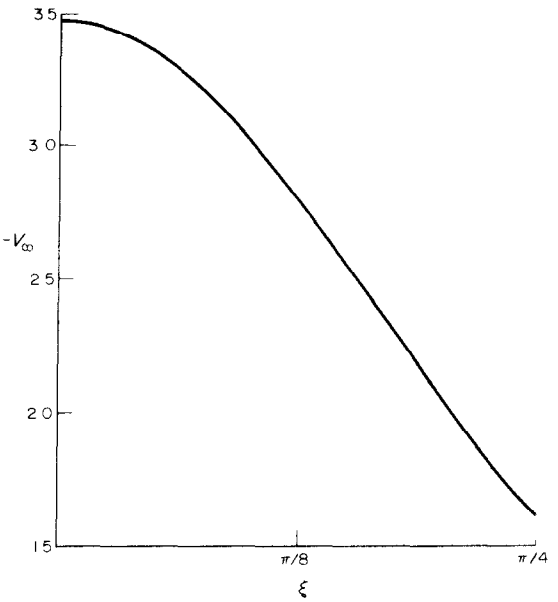

FIG. 8. The radial velocity associated with the steady streaming, at the edge of the outer velocity boundary layer, $Rs \gg 1$.

conclusively demonstrated here. Before continuing our study of the heat transfer characteristics for $Pr \ll 1$, we note that the outer expansion of the stream function is given by $\bar{\psi}_{10}^{(s)} = f(\xi)$ plus exponentially small terms. This means that (82) is the appropriate equation to all orders in the outer region.

The solution of (82) must match with the inner solution (80) and satisfy

$$\Theta = 0 \text{ as } \hat{\eta} \to \infty. \tag{83}$$

The solution of (82) which satisfies (83) is

$$\Theta = D \exp\{V_\infty \hat{\eta}\}. \tag{84}$$

D is a constant to be determined by matching with the inner solution (80). The inner expansion of Θ expressed in terms of the inner variables $\bar{t}, \bar{\eta}$ is

$$\bar{t}_0^{(s)} \sim D\{1 + PrV_\infty \bar{\eta} + Pr^2 \frac{V_\infty^2}{2} \bar{\eta}^2 + O(Pr^3)\}. \tag{85}$$

Interpreting (85) as the outer boundary condition for $\bar{t}_0^{(s)}$ we expand the inner solution as

$$\bar{t}_0^{(s)} = \bar{t}_{00} + Pr\bar{t}_{01} + Pr^2\bar{t}_{02} + O(Pr^3), \tag{86}$$

with the expansion of the outer solution now taking the form

$$D = D_0 + PrD_1 + Pr^2D_2 + O(Pr^3),$$

since (82) is appropriate to all orders. Matching the solutions (80) and (84) to $O(1)$ gives $Q_0 = 0$, $D_0 = 1$ and so $\bar{t}_{00} = 1$. With this unstructured form for $\bar{t}_{00}$, $\bar{t}_{01}$ also satisfies (79) but with $\bar{t}_{01} = 0$ on $\bar{\eta} = 0$, and so matching to $O(Pr)$ gives $D_1 = 0$ and $\bar{t}_{01} = V_\infty\bar{\eta}$. Thus

$$\bar{t}_0^{(s)} = 1 + PrV_\infty\bar{\eta} + O(Pr^2). \tag{87}$$

The equation for $\bar{t}_{02}$, found by substituting (86) into equation (68) and equating coefficients of Pr^2, is

$$\frac{\partial\bar{\psi}_{10}^{(s)}}{\partial\bar{\eta}}\frac{\partial V_\infty}{\partial\xi}\bar{\eta} - \frac{\partial\bar{\psi}_{10}^{(s}}{\partial\xi}V_\infty = \frac{\partial^2\bar{t}_{02}}{\partial\bar{\eta}^2}. \tag{88}$$

Since we are primarily concerned with the behaviour of $(\partial\bar{t}_{02}/\partial\bar{\eta})_{\bar{\eta}=0}$, we integrate equation (88) once with respect to $\bar{\eta}$ from $\bar{\eta} = 0$ to $\bar{\eta} = \infty$, to give

$$\left(\frac{\partial\bar{t}_{02}}{\partial\bar{\eta}}\right)_{\bar{\eta}=0} = V_\infty\int_0^\infty\left[V_\infty + \frac{\partial\bar{\psi}_{10}^{(s)}}{\partial\xi}\right]d\bar{\eta} - V_\infty'\int_0^\infty \frac{\partial\bar{\psi}_{10}^{(s)}}{\partial\bar{\eta}}\bar{\eta}\,d\bar{\eta}. \tag{89}$$

In deriving equation (89) we have used the condition

$$\frac{\partial\bar{t}_{02}}{\partial\bar{\eta}} \sim V_\infty^2 \text{ as } \bar{\eta} \to \infty, \tag{90}$$

which ensures that $\bar{t}_{02}$ matches with the outer solution (84). We numerically evaluate the integrals in (89) using the computed results obtained earlier for $u^{(s)} = \partial\bar{\psi}_{10}^{(s)}/\partial\bar{\eta}$ and $v^{(s)} = -\partial\bar{\psi}_{10}^{(s)}/\partial\xi$. The resulting two term Nusselt number, obtained from the first three terms of (86) using equations (37), (54) and (81) is

$$\frac{Nu}{Rs^{\frac{1}{2}}} = 2{\cdot}71\,Pr - 5{\cdot}51\,Pr^2 + O(Pr^3). \tag{91}$$

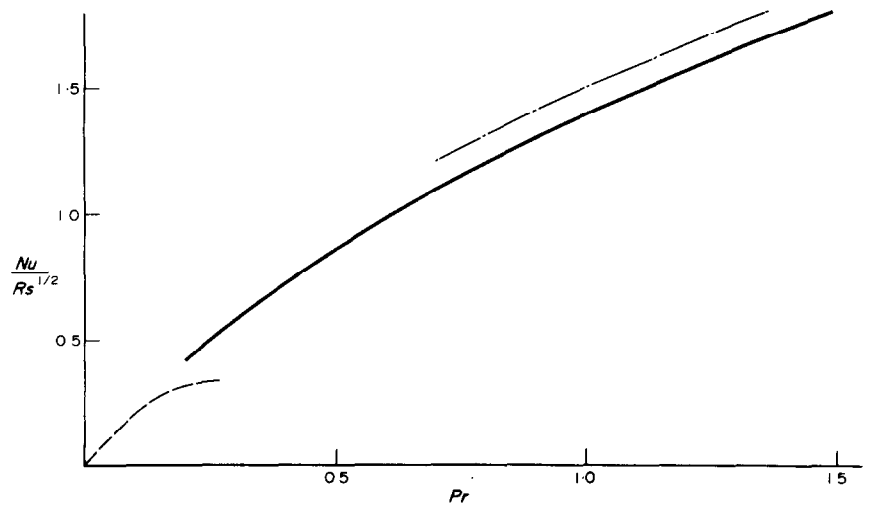

FIG. 9. The computed Nusselt number, ——, together with the asymptotic solutions (78), —·—; and (79), — —, for $Pr \gg 1$. $Pr \ll 1$ respectively for $Rs \gg 1$.

The computed Nusselt number together with the asymptotic solutions (78) and (91) for $Pr \gg 1$ and $Pr \ll 1$ respectively are plotted in Fig. 9 as a function of Pr. It can be seen that the computed solution is consistent with the asymptotic solutions. We note in particular the usefulness of (78) which agrees with the finite difference calculations to within less than 1 per cent for $Pr > 7.5$.

Previous to the work reported here, the only estimate that has been made (see [1]) for the local heat transfer when $Rs \gg 1$, is that near the stagnation point given by equation (71). Taking this local result (71) for the heat transfer and assuming that the wall temperature gradient does not deviate far from the cos ϕ-dependence, which we have shown holds, to first order only, for $Pr \gg 1$, Richardson [1] attempts to obtain an upper limit for the Nusselt number for $Rs \gg 1$. The Nusselt numbers based on Richardsons' calculation for $Pr = 0{\cdot}72$ falls below the value calculated here by about 10 per cent. His result in fact yields smaller values than those calculated here for all Pr and consequently, in no sense, can be accepted as an upper bound for Nu.

In the work described so far we have discussed idealized situations, in which the vibrating cylinder is maintained at a uniform temperature, and assessed the heat transfer characteristics. However in more realistic situations the surface temperature may not be uniform and we may, for example, be faced with a situation in which heat is generated internally within the cylinder. In the final section of this paper we discuss such a case, although our model is again a fairly simple one.

6. INTERNAL HEAT GENERATION PROBLEM

All previous sections have dealt with the heat-transfer characteristics associated with a uniformly heated surface. This situation could be realised quite simply in practice by passing a heated liquid through a thin walled tube. However other situations may arise in which heat is generated internally, such as heat generation by chemical reaction or radioactive decay. In these situations an internal heat-conduction problem must then be solved simultaneously with the external fluid flow problem. The simplest possible situation of this kind, which we discuss here, is one in which heat is produced by a line source at $r = 0$, realisable for example by passing an electric current through a wire, which is embedded along the axis of the solid cylinder. We assume that the total flow of heat per unit length of the wire is uniform.

For this problem we take, as a particular example, the external fluid flow to be that which was discussed in Section 5 which is appropriate for large streaming Reynolds numbers. The temperature distribution in the external region is thus governed by the boundary-layer equation (68), and consequently a mixed parabolic (exterior), elliptic (interior) problem is to be solved. We now describe the method devised to calculate the steady temperature distribution within the cylinder under these circumstances. The calculation outside the cylinder is closely related to that described in Section 5.

Since we are no longer insisting that the wall temperature $\tilde{T}_\omega$ remains constant, we non-dimensionalize temperatures in the equations which are to follow by setting

$$T = \frac{\tilde{T} - \tilde{T}_\omega}{\{Q/2\pi k_1\}}, \tag{92}$$

where Q is the total heat flux per unit length from the wire, which we assume is constant, and k_1 is the thermal conductivity of the solid cylinder. We identify the steady part, with which we are concerned, of the dimensionless temperature within the cylinder by T_i. Then, since T_i must satisfy Laplace's equation, $T_i(r, \phi)$ for this two-dimensional problem is a solution of

$$\frac{\partial^2 T_i}{\partial r^2} + \frac{1}{r}\frac{\partial T_i}{\partial r} + \frac{1}{r^2}\frac{\partial^2 T_i}{\partial \phi^2} = 0. \tag{93}$$

For a line source of heat at the origin $r = 0$, the boundary condition which must be satisfied by T_i is

$$r\frac{\partial T_i}{\partial r} = -1 \text{ on } r = 0. \tag{94}$$

We recall that the governing energy equation in the external region is given by (68) where $\bar{\eta} = Rs^{\frac{1}{2}}(r-1)/2$, together with a boundary condition

$$\bar{t}_0^{(s)} = 0 \text{ as } \bar{\eta} \to \infty, \tag{95}$$

and a condition at $\xi = 0$ derived from (71). If k_2 is the thermal conductivity of the fluid, then the boundary conditions which we apply at the change of medium $r = 1$, at which there is complete thermal contact, are

$$\left.\begin{aligned} T_i(r,\phi) &= \bar{t}_0^{(s)}(\bar{\eta},\xi), \\ k_1\frac{\partial T_i}{\partial r} &= \frac{k_2 Rs^{-\frac{1}{2}}}{2}\frac{\partial \bar{t}_0^{(s)}}{\partial \bar{\eta}}, \end{aligned}\right\} \quad \text{on } r = 1\ (\bar{\eta} = 0) \tag{96}$$

where the latter boundary condition ensures that the heat flux is continuous over the surface of contact. The problem posed by (68) and equations (93)–(96) is now well defined and we next describe the method of solution.

In view of the linking of the exterior problem of parabolic nature and the elliptic interior problem, by the conditions (96), we adopt an iterative method of solution. This is based upon the fact that from the solution in either region that in the other may be determined. We restrict our attention to the single case $Pr = 1{\cdot}0$ and we begin by describing separately the methods by which the solutions in each region are determined.

Equation (93) together with the boundary condition (94) admits a solution of the form

$$T_i = -\log_e r + \Phi(r,\phi), \tag{97}$$

where we require that Φ be finite at $r = 0$. For a circular cylindrical geometry, Φ may be conveniently written as

$$\Phi = \sum_{n=0}^{\infty} r^n\{a_n \cos n\phi + b_n \sin n\phi\}. \tag{98}$$

If we now set $T_i(1,\phi) = G(\phi)$, then from the symmetry which this problem displays about the lines $\phi = 0,\ \pi/2$, $G(\phi)$ has the following properties (i) $G(\phi) = G(-\phi)$, (ii) $G(\phi) = G(\phi+\pi)$ from which we deduce that $b_n \equiv 0$ and $a_{2n+1} \equiv 0$ for all n in equation (98). Consequently we find

$$G(\phi) = a_0 + \sum_{n=1}^{\infty} a_{2n}\cos 2n\phi. \tag{99}$$

Applying the standard Fourier analysis techniques to $G(\phi)$, we have

$$\left.\begin{aligned} a_0 &= \frac{2}{\pi}\int_0^{\pi/2} G(t)\,dt, \\ a_{2n} &= \frac{4}{\pi}\int_0^{\pi/2} G(t)\cos 2nt\,dt. \end{aligned}\right. \tag{100}$$

Thus, if $G(\phi)$ is known, the solution for the interior region is easily found.

If for the exterior region, the derivative $(\partial \bar{t}_0^{(s)}/\partial\bar{\eta})_{\bar{\eta}=0}$ is known, we may, using (71), solve equation (68) appropriate to the exterior region in the manner described in Section 5 using finite difference techniques.

An obvious iterative procedure now presents itself. From the solution in the exterior region we may determine $\bar{t}_0^{(s)}$ on $\bar{\eta} = 0$ which in view of the boundary condition (96) renders the solution of (93) determinate in the interior, as above. From the boundary condition (96b) we then take, as the next approximation to $(\partial \bar{t}_0^{(s)}/\partial\bar{\eta})_{\bar{\eta}=0}$,

$$\left(\frac{\partial \bar{t}_0^{(s)}}{\partial\bar{\eta}}\right)_{\bar{\eta}=0} = \frac{2k_1 Rs^{-\frac{1}{2}}}{k_2}\left(\frac{\partial T_i}{\partial r}\right)_{r=1} = \frac{2k_1 Rs^{-\frac{1}{2}}}{k_2}(1 - \sum_{n=1}^{\infty} 2na_{2n}\cos 2n\phi), \tag{101}$$

from (97) and (98), where the coefficients a_{2n} are given by (100) using the newly calculated values for $G(\phi)$. Using (101) as the next approximation for the wall temperature gradient, the above operations are then repeated. The iterative scheme, may be initiated in a fairly arbitrary manner and is terminated when the absolute value of the sum of the differences of $G(\phi)$ at the $(j+1)$th and jth cycle is less than some prescribed tolerance.

An important parameter in this scheme is the dimensionless quantity $2k_1Rs^{-\frac{1}{2}}/k_2$ which appears explicitly in (101). Since we are restricting the analysis to $Pr = O(1)$ which is true for most gases, we take air, in which $k_2 = 6 \times 10^{-5}$ cal/cm^2 s °C/cm as a typical example. We then find that we may vary the ratio k_1/k_2 from as large as 2×10^3 for metallic cylinders to $k_1/k_2 = O(1)$ for non-metallic materials. We recall however that for the velocity field we have chosen to use in the exterior problem, the associated streaming Reynolds number is large. Consequently for this model, for self-consistency within the framework of our limit processes, we choose values of $2k_1Rs^{-\frac{1}{2}}/k_2$ which are small compared to unity.

During the course of the computation for this particular example it was found that for values of $2k_1Rs^{-\frac{1}{2}}/k_2$ no larger than 0·2, the resulting Fourier series for $G(\phi)$ in (99) converged very slowly and unless more than thirty terms in (99) are included, which demands a very fine mesh size in the ϕ-direction, the equation (99) is an inadequate representation of $G(\phi)$. For details of the technique used to improve the convergence of (99), which are based upon methods due to Shanks [12], and which enable a larger range of $2k_1Rs^{-\frac{1}{2}}/k_2$ to be considered, reference may be made to [10].

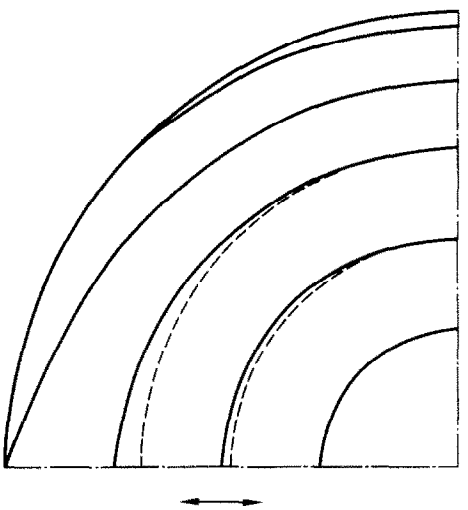

FIG. 10. Isotherms within the cylinder for $2k_1Rs^{-\frac{1}{2}}/k_2 = 0{\cdot}5$. $Rs \gg 1$. The axis of oscillation is indicated and the broken lines represent circular arc segments.

As a particular example, we show in Fig. 10 the isotherms within the cylinder for the case $2k_1Rs^{-\frac{1}{2}}/k_2 = 0{\cdot}5$. This figure shows very well the distortion of the isotherms near $r = 1$ from the concentric circles which we may expect if there were no motion in the exterior region. As we approach the heat source at $r = 0$ the effects of the convective velocities in the exterior region become undetectable, and the isotherms do indeed revert to their familiar circular shapes. We also display in Fig. 11 the values of $\bar{t}_0^{(s)}$ and $\partial\bar{t}_0^{(s)}/\partial\bar{\eta}$ at $\bar{\eta} = 0$ in the solution for this case which was achieved after fifteen iterations to yield accuracy to three significant figures.

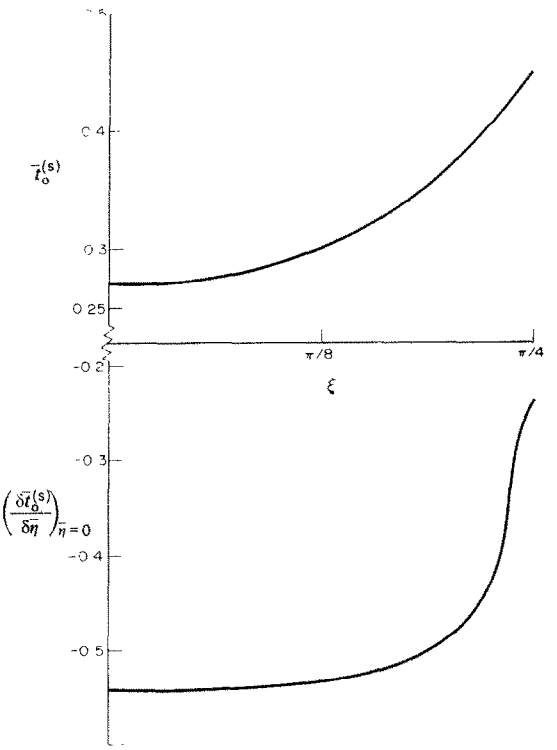

FIG. 11. Profiles of temperature and temperature gradient at the wall as a function of ξ for $2k_1Rs^{-\frac{1}{2}}/k_2 = 0{\cdot}5$. $Rs \gg 1$.

ACKNOWLEDGEMENTS

This work was carried out whilst the author was in receipt of an S.R.C. research studentship. The author wishes to thank Professor N. Riley for helpful guidance and discussion.

REFERENCES

1. P. D. Richardson, Heat transfer from a circular cylinder by acoustic streaming, *J. Fluid Mech.* **30**, 337–355 (1967).
2. N. Riley, Oscillatory viscous flows. Review and extension, *J. Inst. Math. & Applics* **3**, 419–434 (1967).
3. J. T. Stuart, Double boundary layers in oscillatory viscous flow, *J. Fluid Mech.* **24**, 673–687 (1966).
4. M. S. Longuet-Higgins, Mass transport in water waves, *Phil. Trans. R. Soc.* (A) **245**, 535–581 (1953).
5. M. D. Van Dyke, *Perturbation Methods in Fluid Mechanics*. Academic Press, New York (1964).
6. B. J. Davidson, Mass transfer due to cavitation microstreaming, *J. Sound Vibr.* **17**, 261–270 (1971).
7. C. R. Robertson and A. Acrivos, Low Reynolds number shear flow, Part 2, *J. Fluid Mech.* **40**, 717 (1970).
8. R. Grimshaw, On steady recirculating flows, *J. Fluid Mech.* **39**, 695–703 (1969).
9. N. Riley, Oscillating viscous flows, *Mathematika* **12**, 161–175 (1965).
10. B. J. Davidson, Ph.D. Thesis, University of East Anglia (1971).
11. M. Abramowitz and I. A. Stegun, *Handbook of Mathematical Functions*. Dover, New York (1965).
12. D. Shanks, Non-linear transformations of divergent and slowly convergent sequences, *J. Math. Phys.* **34**, 1–42 (1955).
13. B. J. Davidson and N. Riley, Jets induced by oscillating motion, *J. Fluid Mech.* **53**, 287–303 (1972).

APPENDIX

The integrated form of the momentum equation in (58) upon which we base our approximate method is

$$\frac{\mathrm{d}}{\mathrm{d}\xi}\int_0^\infty u^{(s)2}\,\partial\bar{\eta} = -\left(\frac{\partial u^{(s)}}{\partial\bar{\eta}}\right)_{\bar{\eta}=0}. \tag{A.1}$$

Profiles for $u^{(s)}$ are assumed as follows

$$u^{(s)} = \bar{u}\{a\mathrm{e}^{-\bar{\eta}/\delta} + b\mathrm{e}^{-2\bar{\eta}/\delta} + c\mathrm{e}^{-3\bar{\eta}/\delta}\}, \tag{A.2}$$

where $\bar{u} = 3\sin 4\xi$. The unknowns $a(\xi)$, $b(\xi)$, $c(\xi)$ and $\delta(\xi)$ are to be determined by requiring that (A.1) is satisfied and that the following conditions are also satisfied

$$u^{(s)} = 0, \frac{\partial^m u^{(s)}}{\partial\bar{\eta}^m} = 0\,(m = 1, 2\ldots)\text{ as }\bar{\eta}\to\infty,$$

$$u^{(s)} = \bar{u}, \frac{\partial^2 u^{(s)}}{\partial\bar{\eta}^2} = \bar{u}\frac{\partial u^{(s)}}{\partial\xi}\text{ on }\bar{\eta} = 0, \tag{A.3}$$

$$\frac{\partial^3 u^{(s)}}{\partial\bar{\eta}^3} = \bar{u}\frac{\partial^2 u^{(s)}}{\partial\xi\partial\bar{\eta}}\text{ on }\bar{\eta} = 0\,. \tag{A.4}$$

The conditions at infinity are trivially satisfied by (A.2); the compatibility conditions (A.3b) and (A.4) are derived from the basic momentum equation in (58). From (A.3) we require

$$b = \tfrac{1}{3}(\lambda - 1 - 8c),\ a = \tfrac{1}{3}(4 - \lambda + 5c), \tag{A.5}$$

and from (A.4)

$$\bar{u}\frac{\partial z}{\partial\xi}t_1 + \bar{u}\bar{u}_{\xi\xi}z^2 - 2\bar{u}z\frac{\partial c}{\partial\xi} = t_2, \tag{A.6}$$

where

$$t_1 = \lambda - \tfrac{1}{2}(2 + \lambda - 2c),$$
$$t_2 = 2c(\lambda + 11) - (\lambda - 1)(\lambda - 4), \tag{A.7}$$

and

$$z = \delta^2 = \frac{\lambda}{\bar{u}_\xi}\,.$$

Substituting (A.2) into (A.1) we have the further equation,

$$u\frac{\partial z}{\partial\xi}t_3 + \bar{u}\bar{u}_{\xi\xi}z^2t_4 + \bar{u}zt_5\frac{\partial c}{\partial\xi} = t_6, \tag{A.8}$$

where

$$t_3 = \tfrac{1}{216}(57 - 42\lambda + 5\lambda^2) + \tfrac{1}{540}(124c - 57c\lambda + 37c^2),$$
$$t_4 = \tfrac{1}{54}(\lambda - 7) + \frac{19c}{270},$$
$$t_5 = \tfrac{1}{270}(124 + 74c - 19\lambda), \tag{A.9}$$
$$t_6 = \tfrac{1}{270}(180 - 245\lambda + 70\lambda^2 - 5\lambda^3 - 180c - 248\lambda c + 38\lambda^2 c - 74\lambda c^2).$$

The equations (A.6) and (A.8) have to be integrated numerically from $\xi = 0$ to determine z and c; a and b then follow from (A.5). For a boundary layer starting from a stagnation point we require that z_ξ and c_ξ remain finite so that $t_2 = t_6 = 0$ when $\bar{u} = 0$. It therefore follows from (A.7) that

$$c = \frac{(\lambda - 1)(\lambda - 4)}{2(\lambda + 11)}\text{ at }\xi = 0. \tag{A.10}$$

Substituting this value of c into (A,9) we find that the only physically acceptable root of $t_6(\lambda) = 0$ is $\lambda = 1{\cdot}0$ and so from (A.7) and (A.10),

$$z(0) = \tfrac{1}{12}, \qquad c(0) = 0{\cdot}0. \tag{A.11}$$

We solve equations (A.6) and (A.8) subject to the boundary conditions (A.11) using a fourth order Runge Kutta process. The displacement thickness δ_1/ξ and the shear stress τ_0 at the inner edge of the outer boundary layer are found by substituting the assumed profile (A.2) into equations (65) and (66) respectively to give

$$\frac{\delta_1}{\{2aRs^{-\frac{1}{2}}\}} = \frac{\delta}{6}(7 - \lambda + 4c),$$
$$\frac{\tau_0}{\frac{\{\mu U_\infty Rs^{\frac{1}{2}}\}}{4a}} = \frac{-\bar{u}}{3\delta}(2 + \lambda - 2c). \tag{A.12}$$

The integral form of the energy equation (68) is

$$\frac{\mathrm{d}}{\mathrm{d}\xi}\int_0^\infty u^{(s)}\bar{t}_0^{(s)}\,\mathrm{d}\bar{\eta} = -\frac{1}{Pr}\left(\frac{\partial \bar{t}_0^{(s)}}{\partial \bar{\eta}}\right)_{\bar{\eta}=0}. \tag{A.13}$$

Exponential profiles for $\bar{t}_0^{(s)}$ are assumed as follows

$$\bar{t}_0^{(s)} = d\,\mathrm{e}^{-\bar{\eta}\cdot\delta_t} + e\,\mathrm{e}^{-2\bar{\eta}\cdot\delta_t} + f\,\mathrm{e}^{-3\bar{\eta}\cdot\delta_t}, \tag{A.14}$$

where the unknowns $d(\xi)$, $e(\xi)$, $f(\xi)$ and $\delta_t(\xi)$ are to be determined by requiring that (A.13) be satisfied and that the following conditions are also satisfied

$$\bar{t}_0^{(s)} = 0, \quad \frac{\partial^m \bar{t}_0^{(s)}}{\partial \bar{\eta}^m} = 0 \quad (m = 1, 2\ldots) \text{ as } \bar{\eta} \to \infty,$$
$$\bar{t}_0^{(s)} = 1, \quad \frac{1}{Pr}\frac{\partial^2 \bar{t}_0^{(s)}}{\partial \bar{\eta}^2} = \bar{u}\frac{\partial \bar{t}_0^{(s)}}{\partial \xi} \text{ on } \bar{\eta} = 0, \tag{A.15}$$

$$\frac{1}{Pr}\frac{\partial^3 \bar{t}_0^{(s)}}{\partial \bar{\eta}^3} = \frac{\partial u^{(s)}}{\partial \bar{\eta}}\frac{\partial \bar{t}_0^{(s)}}{\partial \xi} + \bar{u}\frac{\partial^2 \bar{t}_0^{(s)}}{\partial \xi \partial \bar{\eta}} - \bar{u}'\frac{\partial \bar{t}_0^{(s)}}{\partial \bar{\eta}} \text{ on } \bar{\eta} = 0. \tag{A.16}$$

The conditions at infinity are trivially satisfied by (A.14); the compatibility conditions (A.15b) and (A.16) are derived from the energy equation (68). From (A.15) we require

$$d = \tfrac{1}{3}(4 + 5f), \quad e = \tfrac{1}{3}(8f - 1), \tag{A.17}$$

and from (A.16), using (A.7c),

$$\frac{\partial f}{\partial \xi} = -(1 - f)\left\{\frac{1}{2\lambda}\left(z\bar{u}'' + z'\bar{u}' + \frac{\lambda}{\Delta^2}\frac{\partial}{\partial \xi}(\Delta^2) - \frac{\lambda \bar{u}''}{\bar{u}'}\right) + \frac{\bar{u}'}{\bar{u}}\right\} + \frac{(2 - 11f)\bar{u}'}{\Delta^2 \lambda \bar{u}\, Pr} \tag{A.18}$$

where $\Delta = \delta_t/\delta$ substituting the velocity and temperature profiles given by (A.2) and (A.14) respectively in (A.13) we have the further equation

$$\frac{\partial}{\partial \xi}(\Delta^2) + \Delta^2\left\{\frac{z\bar{u}''}{\lambda} + \frac{\bar{u}'z'}{\lambda} - \frac{\bar{u}''}{\bar{u}'} + \frac{2\bar{u}'}{\bar{u}} + \frac{2}{H}\frac{\partial H}{\partial \xi}\right\} = \frac{4\bar{u}'(1 - f)}{3\bar{u}H\lambda\, Pr}, \tag{A.19}$$

where

$$H = a\left(\frac{d}{1 + \Delta} + \frac{e}{2 + \Delta} + \frac{f}{3 + \Delta}\right) + b\left(\frac{d}{1 + 2\Delta} + \frac{e}{2 + 2\Delta} + \frac{f}{3 + 3\Delta}\right) + c\left(\frac{d}{1 + 3\Delta} + \frac{e}{2 + 3\Delta} + \frac{f}{3 + 3\Delta}\right), \tag{A.20}$$

and a, b, d and e are given in (A.5) and (A.17). Equations (A.18) and (A.19) have to be integrated numerically, simultaneously with equations (A.6) and (A.8), to determine f; Δ^2; d and e then follow from (A.17). To integrate (A.18) and (A.19) starting from the stagnation point $\xi = 0$ we require f_ξ and Δ_ξ^2 to remain finite at $\xi = 0$. It therefore follows from (A.18) and (A.19) that

$$\left.\begin{aligned}(1 - f) &= \frac{9}{(11 - Pr\,\Delta^2)}\\ \Delta^2 &= \frac{2(1 - f)}{3Pr\,H}\end{aligned}\right\} \quad \text{at } \xi = 0, \tag{A.21}$$

respectively. For $Pr = 1{\cdot}0$, we find that on eliminating f in (A.21) and solving the resulting sixth degree equation in Δ, the only physically acceptable root is

$$\Delta = 1{\cdot}037382, \tag{A.22}$$

so that

$$f = 0{\cdot}093093.$$

Equations (A.6), A(8), (A.18) and (A.19) are solved together with the boundary conditions (A.11) and (A.22) using a fourth order Runge-Kutta process. Values for the local heat transfer $(\partial \bar{t}_0^{(s)}/\partial \bar{\eta})_{\bar{\eta}=0}$ are then found from the expression

$$\left(\frac{\partial \bar{t}_0^{(s)}}{\partial \bar{\eta}}\right)_{\bar{\eta}=0} = \frac{2(1 - f)}{3\Delta z^{\frac{1}{2}}}.$$

TRANSFERT THERMIQUE PAR UN CYLINDRE VERTICAL VIBRANT

Résumé—On a obtenu des résultats théoriques pour le transfert thermique par un cylindre circulaire oscillant dans un fluide visqueux illimité au repos. L'amplitude de l'oscillation est supposée petite comparée au rayon du cylindre, qui, pour la plupart des exemples considérés, est supposé être à la température constante. L'analyse est basée sur l'utilisation du champ dynamique acoustique et les cas de petits et grands nombres de Reynolds de l'écoulement sont considérés. Pour de grands nombres de Reynolds, il a été calculé une solution pour le champ d'écoulement permanent non déterminé antérieurement. Les résultats obtenus couvrent un large domaine du nombre de Prandtl. La méthode des développements asymptotiques est exploitée dans l'analyse et les résultats calculés sont également complétés par une méthode approchée basée sur une forme intégrée des équations de base. La relation entre le travail présenté

et d'autres contributions correspondantes déjà publiées est discutée. Dans une section finale l'attention est portée sur une technique de détermination de la distribution de température pour une source linéaire de chaleur placée au centre du cylindre oscillant.

WÄRMEÜBERTRAGUNG VON EINEM VIBRIERENDEN KREISZYLINDER

Zusammenfassung—Theoretische Ergebnisse wurden für die Wärmeübertragung von einem kreisförmigen Zylinder erhalten, der in einer unbegrenzten sonst ruhigen viskosen Flüssigkeit oszillierte. Die Schwingungsamplitude soll klein gegenüber dem Zylinderradius sein.

Die Zylindertemperatur wurde für die betrachteten Beispiele als konstant angenommen.

Die Analysis basiert auf dem akustischen Strömungsfeld. Fälle von kleinen und großen Reynolds-Zahlen werden betrachtet. Für große Reynolds-Zahlen wird eine Lösung für das bisher unbestimmte stationäre Strömungsfeld berechnet. Die erhaltenen Ergebnisse überdecken einen grossen Bereich der Prandtl-Zahl. Die Methode der asymptotischen Entwicklungen wird in der Analysis ausgenutzt, und auch die berechneten Ergebnisse werden durch eine Näherungsmethode ergänzt, die auf einer integrierten Form der Hauptgleichungen basiert. Die Beziehungen zwischen der vorliegenden Arbeit und anderen entsprechenden Beiträgen in der Literatur werden erörtert. In einem Schlußabschnitt wird zur Bestimmung der Temperaturverteilung eine Technik verwendet, die sich ergibt, wenn eine linienförmige Wärmequelle im Zentrum eines schwingenden Zylinders liegt.

ПЕРЕНОС ТЕПЛА ОТ ВИБРИРУЮЩЕГО КОЛЬЦЕВОГО ЦИЛИНДРА

Аннотация—Получены теоретические результаты по исследованию процесса переноса тепла от кольцевого цилиндра, колеблющегося в неограниченной вязкой жидкости, находившейся в состоянии покоя. Предполагается, что амплитуда колебания мала по сравнению с радиусом цилиндра, температура которого в большинстве из рассматриваемых примеров принимается постоянной. В основе анализа лежит использование акустической модели поля течения. Рассматриваются случаи малых и больших чисел Рейнольдса набегающего потока. Для больших значений числа Рейнольдса получено численное решение ранее не исследованной задачи о стационаоном поле течения. Результаты получены для широкого диапазона значений числа Прандтля. В анализе использован метод взаимных асимптотических разложений и результаты численного расчета сравнены с результатами приближенного решения интегральным методом. Дается сравнение результатов работы с данными аналогичных работ других авторов. Последняя часть работы посвящена методике определения распределения температуры в случае, когда на оси колеблющегося цилиндра сосредоточен линейным источник тепла.